Bioorganic Chemistry 104 (2020) 104218

Contents lists available at ScienceDirect

Bioorganic Chemistry

journal homepage: www.elsevier.com/locate/bioorg

Design, synthesis, and biological evaluation of new challenging thalidomide analogs as potential anticancer immunomodulatory agents

Mohamed Ayman El-Zahabi[a,*], Helmy Sakr[a], Khaled. El-Adl[a,b], Mohamed Zayed[a,c], Adel S. Abdelraheem[a], Sally I. Eissa[d], Hazem Elkady[a,b], Ibrahim H. Eissa[a,*]

[a] Pharmaceutical Medicinal Chemistry & Drug Design Department, Faculty of Pharmacy (Boys), Al-Azhar University, Cairo 11884, Egypt
[b] Pharmaceutical Chemistry Department, Faculty of Pharmacy, Heliopolis University for Sustainable Development, Cairo, Egypt
[c] Pharmaceutical Sciences Department, Fakeeh College for Medical Sciences, Jeddah 21461, Saudi Arabia
[d] Pharmaceutical Medicinal Chemistry & Drug Design Department, Faculty of Pharmacy (Girls), Al-Azhar University, Cairo, Nasser City, Egypt

ARTICLE INFO

Keywords:
Anticancer
Apoptosis
Immunomodulators
Thalidomide

ABSTRACT

Thalidomide and its analogs are immunomodulatory drugs that inhibit the production of certain inflammatory mediators associated with cancer. In the present work, a new series of thalidomide analogs was designed and synthesized to obtain new effective antitumor immunomodulatory agents. The synthesized compounds were evaluated for their cytotoxic activities against a panel of four cancer cell lines (HepG-2, HCT-116, PC3 and MCF-7). Compounds **33$_h$**, **33$_i$**, **42$_f$** and **42$_h$** showed strong potencies against all tested cell lines with IC_{50} values ranging from 14.63 to 49.90 μM comparable to that of thalidomide (IC_{50} values ranging from 32.12 to 76.91 μM). The most active compounds were further evaluated for their *in vitro* immunomodulatory activities via estimation of human tumor necrosis factor alpha (TNF-α), human caspase-8 (CASP8), human vascular endothelial growth factor (VEGF), and nuclear factor kappa-B *P*65 (NF-κB *P*65) in HCT-116 cells. Thalidomide was used as a positive control. Compounds **33$_h$** and **42$_f$** showed a significant reduction in TNF-α. Furthermore, compounds **33$_i$** and **42$_f$** exhibited significant elevation in CASP8 levels. Compounds **33$_i$** and **42$_f$** inhibited VEGF. In addition, compound **42$_f$** showed significant decrease in levels of NF-κB p65. Moreover, apoptosis and cell cycle tests of the most active compound **42$_f$**, were performed. The results indicated that compound **42$_f$** significantly induce apoptosis in HCT-116 cells and arrest cell cycle at the G2/M phase.

1. Introduction

Thalidomide was formerly recognized as a sedative and it was used for the treatment of morning sickness especially in pregnant women [1]. Nevertheless, its serious teratogenic side effects were reported in 1961 and 1962 [2]. Limb defects (amelia and phocomelia) were the most well-known serious embryotoxic effects caused by the use of thalidomide during early pregnancy [3]. Thalidomide was banned and withdrawn from the market, but many studies have continued to reveal the mechanism of its action [4–7]. Subsequently, thalidomide (**1**) has been shown to be efficacious in the treatment of different diseases, including cancer [8], acquired immunodeficiency syndrome (AIDS) [9], leprosy [9], multiple myeloma [10], and other angiogenesis-dependent disorders [11].

Thalidomide is considered as a prototype of the glutarimide-containing immunomodulatory agents [12]. It inhibits the production of many inflammatory mediators such as tumor necrosis factor-alpha (TNF-α) and can affect the production of the others, such as interleukin-1b (IL-1b), IL-2, IL-4, IL-5, IL-6, IL-10, and interferon- γ (IFN- γ) [11]. Moreover, thalidomide and thalidomide analogs inhibit the secretion of both beta fibroblast growth factor (bFGF) and vascular endothelial growth factor (VEGF) from cancer cells and bone marrow stromal cells, leading to reduction of endothelial cell migration and proliferation and induction of apoptosis [13].

The concept of using thalidomide in the treatment of cancer emerged after the discovery of its antiangiogenic effects in the early 1990s [3]. Although the mechanism of thalidomide in cancer treatment is not fully clear, its analogs have demonstrated immunomodulatory and anti-inflammatory properties in addition to their anti-angiogenic effects [14,15].

Second-generation thalidomide analogs, lenalidomide (**2**), is a potent immunomodulator that is 50,000 times more potent than thalidomide as an inhibitor of TNF-α [16]. Clinical studies have revealed that lenalidomide demonstrates fewer side effects and almost neither

* Corresponding authors.
E-mail addresses: malzahaby@yahoo.com (M.A. El-Zahabi), Ibrahimeissa@azhar.edu.eg (I.H. Eissa).

https://doi.org/10.1016/j.bioorg.2020.104218
Received 26 February 2020; Received in revised form 4 June 2020; Accepted 22 August 2020
Available online 01 September 2020

neurological toxicity nor teratogenicity, compared to thalidomide [17]. Structural modification of thalidomide (**1**) via the addition of an amino group at the 4-position of the phthaloyl ring forming pomalidomide (**3**) which was 10-fold more potent than lenalidomide (**2**) as a TNF-α inhibitor and interleukin-2 (IL-2) stimulator [18]. It also showed better anti-angiogenic results than thalidomide (**1**) and lenalidomide (**2**) [19].

Thalidomide and its analogs have displayed promising activity against a wide variety of diseases, including cancer and inflammatory diseases [20]. The known immunomodulatory and anti-angiogenic properties of thalidomide analogs provided the motivation to explore these agents in the treatment of both hematologic malignancies and solid tumors [8]. Numerous early-phase trials in solid tumors have shown activity in prostate cancer [21], breast cancer [22], Kaposi's sarcoma [23], renal cell cancer [24], melanoma [24], neuroendocrine tumors [25], hepatocellular carcinoma [26], lung cancer, and gliomas [27]. Furthermore, thalidomide and thalidomide analogs are effective agents for the treatment of both lymphoid and myeloid carcinoma with significant activity in non-Hodgkin's lymphoma [28]. Also, thalidomide and thalidomide analogs showed promising activity against acute myeloid leukemia [29] and myelofibrosis with myeloid metaplasia [28].

The recent reported mechanism of thalidomide (**1**), lenalidomide (**2**) and pomalidomide (**3**) as immunomodulatory agents is that these compounds co-stimulate T cells via the degradation of two DNA transcription factors known as Aiolos and Ikaros [30]. In the absence of thalidomide, lenalidomide and pomalidomide, Aiolos and Ikaros are expressed and act as repressors of the IL-2 promoter. The presence of thalidomide, lenalidomide and pomalidomide increases the interaction of cereblon (CRBN) with Aiolos and Ikaros, causing their ubiquitination and degradation resulting in de-repression of the IL-2 promoter and increased expression of IL-2 [30].

In this work, thalidomide (**1**) was selected a lead compound for the synthesis of new anticancer agents with immunomodulatory activities. The synthesized compounds were designed to have the main essential pharmacophoric features of thalidomide and its analogs. The structures of thalidomide analogs consist of glutarimide and phthalimide moieties.

It was found that, thalidomide can be a guide for our design, because it has the following criteria. i) Immunomodulation: It can co-stimulate *T*-cells resulting in synthesis of specific *T*-killer cells which target the cancer cells [31]. ii) The common side effects of cytotoxic anticancer agents were not reported for thalidomide [32]. iii) Different mechanisms were reported for thalidomide as anticancer drug [33]. Beside immunomodulation, it was reported to cause ubiquitination of Ikaros and Aiolos, resulting in apoptosis and arresting cell life cycle [34]. It also was reported to have anti-angiogenic activity by inhibition of both VEGF and bFGF-2 [35]. Moreover, it inhibits the adhesion between tumor cells and stromal cells preventing signals which stimulate tumor cells survival, growth and development of drug resistance [36]. iv) The teratogenicity of thalidomide was reduced in rabbit model via structural modification to produce lenalidomide with higher anticancer activity [12].

1.1. Rationale of molecular design

For many years, our research group have many efforts to design and synthesize new compounds with potential anticancer effect [37–47]. As extension for such efforts, we carried out this work. Studying the structure-activity relationship of thalidomide analogs (thalidomide (**1**), lenalidomide (**2**) and pomalidomide (**3**)), it was found that they have four common essential pharmacophoric features. These features include: i) hydrophobic domain, ii) five membered ring, iii) spacer, and iv) glutarimide moiety (Fig. 1).

By literature survey, it was found that there are many efforts to modify thalidomide with the primary aim of obtaining more effective new immunomodulatory agents free from harmful effects.

Briefly, replacement of the glutarimide moiety of thalidomide with *β*-aryl carboxamide derivative **4** and *β*-aryl acetate derivative **5** resulted in significant inhibition of TNF-α by 500 times that exhibited by thalidomide [48]. Other modifications were carried out by replacement of the glutarimide moiety with phenyl ring to produce new compounds with promising biological activity. For example, compounds **6** and **7** demonstrated improved anti-angiogenic and cancer activities [49,50]. Furthermore, variation of alkyl substituents strategy was performed to get compound **8** as a modified thalidomide analog. Such compound produced comparable TNF-α inhibitory effect to thalidomide [51]. Moreover, molecular hybridization of phthaloyl nucleus and 1,3,4-thiadiazole moiety produced compound **9** which exhibited a significant cytotoxic effect against HepG-2 cells comparable to thalidomide [52].

There is another pathway that has been taken to modify thalidomide via the extension of extra functional groups strategy. Such extension was carried out on the glutarimide moiety through the insertion of dithiocarbamate derivative to produce compound **10**. This compound exhibited *in vitro* antitumor activity against an ascites carcinoma cell line [53]. In 2009, Brana *et al,* synthesized compound **11** via ring variation pathway, where the phthaloyl nucleus of thalidomide was replaced by diphenylmaleimide moiety. Such compound showed a strong inhibitory activity for TNF-α production [54].

Dramatic modifications of thalidomide were carried out to give compound **12**, **13**, and **14**, where the phthaloyl nucleus was replaced by 4,9-dihydro-2*H*-[1,2,5]thiadiazolo[2,3-*b*]isoquinolin-3(3a*H*)-one 1,1-dioxide in compound **12**, 1-(phenylsulfonyl)-1*H*-pyrrolo[2,3-*b*]pyridine in compound **13**, and 2-carboxybenzamide in compound **14**. TNF-α inhibitory effect and IL-10 stimulatory effect were reported *in vitro* on account of these derivatives (Fig. 2) [55,56].

On the other side, bioisosteric modifications of thalidomide were accomplished by replacement the glutarimide moiety by many bioisosteres such as benzimidazole, benzothiazole, benzothiadiazole, urea, thiourea, and thiazolidinone derivatives to afford compounds **15**, **16, 17**, **18**, **19**, and **20**, respectively. Such derivatives showed promising antiangiogenic potential, and compound **20** revealed immunosuppressive effect [57–59].

Additionally, the potential anticancer activity of some bioactive moieties was explored. 1,3,4-Oxadiazole nucleus was proven to have potential anticancer effect [60,61]. Compounds **21** and **22** as examples of compounds containing 1,3,4-oxadiazole moiety showed *in vitro* anticancer activity against breast cancer (MCF-7) cell line. Thiazolidine-2,4-dione is another example of interesting bioactive moieties having potential anticancer effect. Compounds **23**, **24** and **25** incorporated such moiety were reported to possess *in vitro* anti-breast cancer activity (Fig. 2) [62].

Depending on the previously mentioned structural modification and ligand-based drug design approach, we used thalidomide **1** as a lead compound to get new effective immunomodulatory anticancer agents. The rational of molecular design was based on molecular hybridization strategy which involves the coupling of two or more groups with relevant biological properties to produce new compounds with promising activities [63,64]. Accordingly, the aminopiperidinedione moiety was hybridized with thiazolidinedione derivatives to produce (Scaffold-I), and with oxadiazole derivatives to obtain (Scaffold-II) (Fig. 3).

The main core of our molecular design rationale comprised molecular modification of thalidomide at three different positions (Fig. 4). The first position was the phenyl ring; where different substituted phenyl derivatives were used. The substituted phenyl derivatives may be directly attached to heterocyclic ring as compounds $\mathbf{42_{a\text{-}i}}$ or separated by one carbon-bridge as compounds $\mathbf{33_{a\text{-}j}}$. The second position was the 1*H*-pyrrole-2,5-dione ring. This five-membered ring was replaced by different rings as thiazolidine-2,4-dione as compounds $\mathbf{33_{a\text{-}j}}$, and 1,3,4-oxadiazole as compounds $\mathbf{42_{a\text{-}i}}$. The third position was the spacer region. The length of the spacer was modified to be three (compounds $\mathbf{33_{a\text{-}j}}$), or four (compounds $\mathbf{42_{a\text{-}i}}$) atom bridges. Such spacers were expected to increase flexibility of the designed compounds.

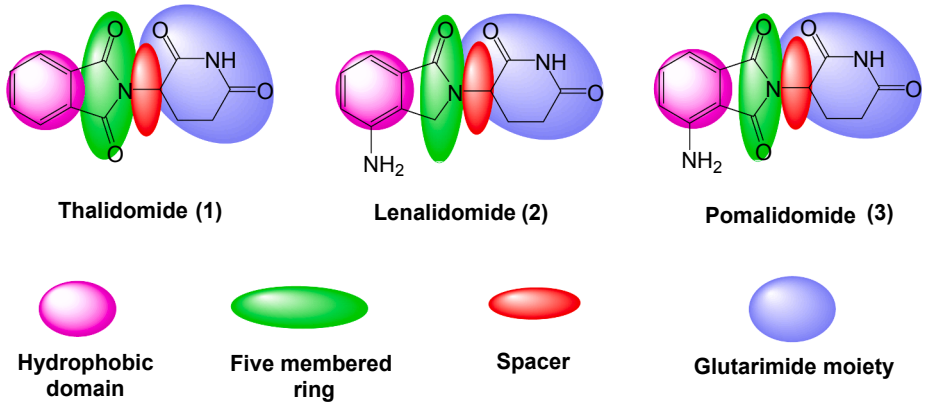

Fig. 1. Pharmacophoric features of thalidomide, lenalidomide, pomalidomide.

As shown in Fig. 5**,** our target compounds have the main the pharmacophoric features of the lead compound (thalidomide).

In general, to examine the cytotoxic effect of the synthesized compounds, they were evaluated *in vitro* against HepG-2, HCT-116, PC3, and MCF-7 cell lines. The reported activities of thalidomide analogs to activate CASP8 and to inhibit TNF-α, VEGF, and NF-κB *P*65 drove us for further examinations to reach a deep insight about the immunomodulatory effect of the synthesized compounds. Hence, the most cytotoxic agents were examined for their immunomodulatory activities via determination of their effect on TNF-α, CASP8, VEGF, and NF-κB *P*65 in HCT-116. Moreover, the effect of the most active compound **42$_f$** on apoptosis and cell cycle was investigated in HCT-116 cell line.

2. Results and discussion

2.1. Chemistry

For synthesis of the target compounds, reactions sequence is clarified in Schemes 1 and 2**.** At first, the starting material thiazolidine-2,4-dione (TZD) **28** was synthesized according to the reported procedures by the reaction of chloroacetic acid **26** with thiourea **27** under reflux in conc. HCl [65]. Condensation of compound **28** with certain aromatic aldehydes namely, benzaldehyde, 2-chlorobenzaldehyde, 4-chlorobenzaldehyde, 2-methoxybenzaldehyde, 4-methoxybenzaldehyde, 4-fluorobenzaldehyde, 4-methylbenzaldehyde, 4-nitobenzaldehyde, 3-nitobenzaldehyde and 2,6-dichlorobenzaldehyde in absolute ethanol with catalytic amount of piperidine yielded the corresponding compounds **29$_{a-j}$**, respectively [65–67]. Subsequent treatment of compounds **29$_{a-j}$** with potassium hydroxide produced the corresponding potassium salts **30$_{a-j}$**, respectively based on the reported procedure of preparation of organic slats [68,69]. Reflux of **30$_{a-j}$** with methyl bromoacetate afforded the corresponding compounds **31$_{a-j}$**, respectively [65,66] which in turn were hydrolyzed in acidic medium providing the corresponding acids **32$_{a-j}$** in high yields [65,66]. The obtained compounds **32$_{a-j}$** were allowed to react with ethyl chloroformate to give the corresponding mixed anhydride. Then, 3-aminopiperidine-2,6-dione HCl reacted with the obtained mixed anhydride to afford the final target compounds **33$_{a-j}$**, respectively (scheme 1).

The IR spectra of **33$_{a-j}$** showed no bands for carboxylic group and demonstrated stretching bands at a range of 3419–3202 cm^{-1} corresponding to NH groups. Moreover, ^{1}H NMR of these compounds exhibited neither signals for carboxylic proton nor signals for free NH_2 of 3-aminopiperidine-2,6-dione. Instead, it showed a signal for single proton at 8.72–8.74 ppm which indicates the presence of amidic proton whereas the imidic proton of glutarimide ring appeared as a singlet signal at a range of δ 10.86–10.88 ppm. Moreover, the two protons of CH_2CO appeared as two multiplet signals around 2.48 and 2.75 ppm due to enantiotropicity [70–72]. Mass spectroscopic analyses for compounds 11b and 11d as representative examples exhibited molecular ion peaks at 407 and 391, respectively.

Ester derivatives **35$_{a-i}$** were prepared according to the reported procedures [73] by refluxing the appropriate acid derivatives (**34$_{a-i}$**) namely, benzoic acid, 2-chlorobenzoic acid, 3-chlorobenzoic acid, 4-chlorobenzoic acid, 4-nitrobenzoic acid, 4-aminobenzoic acid, picolinic acid, nicotinic acid and/or isonicotinic acid in methanol in the presence of sulfuric acid [73]. Reflux of **35$_{a-i}$** with hydrazine hydrate afforded the corresponding acid hydrazides **36$_{a-i}$**. [73] Moreover, reflux of **36$_{a-i}$** in alcoholic mixture of carbon disulphide and potassium hydroxide produced **37$_{a-i}$** [73,74]. The treatment of compounds **37$_{a-i}$** with alcoholic solution of potassium hydroxide afforded potassium salt of 5-(un) substituted aryl-1,3,4-oxadiazole-2-thiol **38$_{a-i}$** [73,74]. On the other hand, compound **41** was produced in two phase system (DCM and water) in the presence of two molar equivalent of $NaHCO_3$ in ice-salt bath. Then, heating a mixture of compound **41** with **38$_{a-i}$** in dry DMF yielded the corresponding target compounds **42$_{a-i}$**, respectively (scheme 2).

IR spectra of compounds **42$_{a-i}$** showed stretching bands at a range of 3360–3198 cm^{-1} corresponding to NH groups. ^{1}H NMR spectra of compounds **42$_{a-i}$** exhibited singlet signals for amidic protons at a range of 8.72–8.74 ppm. Also, singlet signals appeared at range of δ 10.86–10.88 ppm corresponding to the imidic protons. Moreover, the two protons of CH_2CO appeared as two multiplet signals around 2.48 and 2.78 ppm due to enantiotropicity [70–72]. Mass spectroscopic analyses for compounds **42$_b$** and **42$_h$** exhibited molecular ion peaks at 379 and 347, respectively.

2.2. Biological testing

2.2.1. In vitro anti-proliferative activity

The synthesized compounds have been tested for their *in vitro* anticancer activities *via* MTT method [75], against four human tumor cell lines; hepatocellular carcinoma (HepG-2), colorectal carcinoma (HCT-116), prostate cancer (PC3) and mammary gland cancer (MCF-7). The results of cytotoxicity were stated as IC_{50} values and summarized in Table 1.

The cytotoxicity results indicated that the majority of the examined compounds showed anti-proliferative activities against the tested cell lines. In general, compounds **33$_h$, 33$_i$, 42$_f$** and **42$_h$** were the most active members of this study, showing promising anti proliferative activities against HepG-2, HCT-116, PC3 and MCF-7 with IC_{50} far less than the reference compound, thalidomide, (IC_{50} = 61.10 ± 3.8, 32.12 ± 3.2, 76.91 ± 4.2 and 45.76 ± 3.6, respectively). Compound **33$_h$** exhibited cytotoxic activities with IC_{50} values of 21.34 ± 1.8, 29.38 ± 2.8, 42.96 ± 2.9 and 19.62 ± 1.6, respectively. Compound **33$_i$** had cytotoxic activities with IC_{50} values of 23.96 ± 2.0, 36.07 ± 3.2, 49.90 ± 3.4 and 21.82 ± 1.8 μM, respectively. Moreover, compound

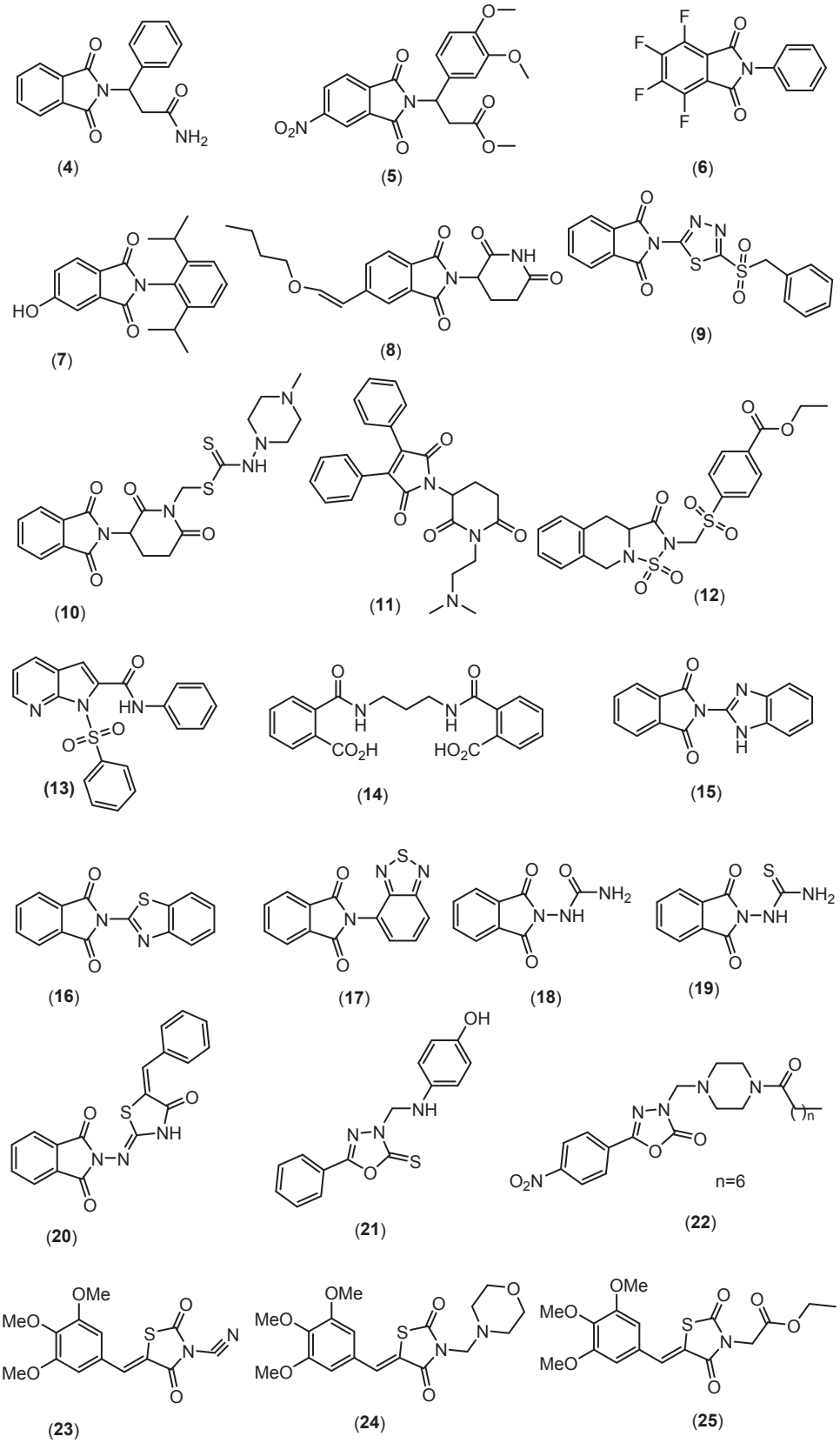

Fig.2. Literature based structures of modified thalidomide analogues and anticancer agents.

42_f revealed IC_{50} values of 16.48 ± 1.6, 23.94 ± 2.3, 28.43 ± 2.0 and 14.63 ± 1.3, respectively. Furthermore, compound **42_h** found to have cytotoxic activities with IC_{50} values of 19.47 ± 1.7, 32.60 ± 2.9, 46.81 ± 3.0 and 18.15 ± 1.5 μM, respectively.

Moreover, several compounds such as **33_a, 33_f, 33_j, 42_e** and **42_i** showed moderate anti-proliferative activities with IC_{50} values ranging

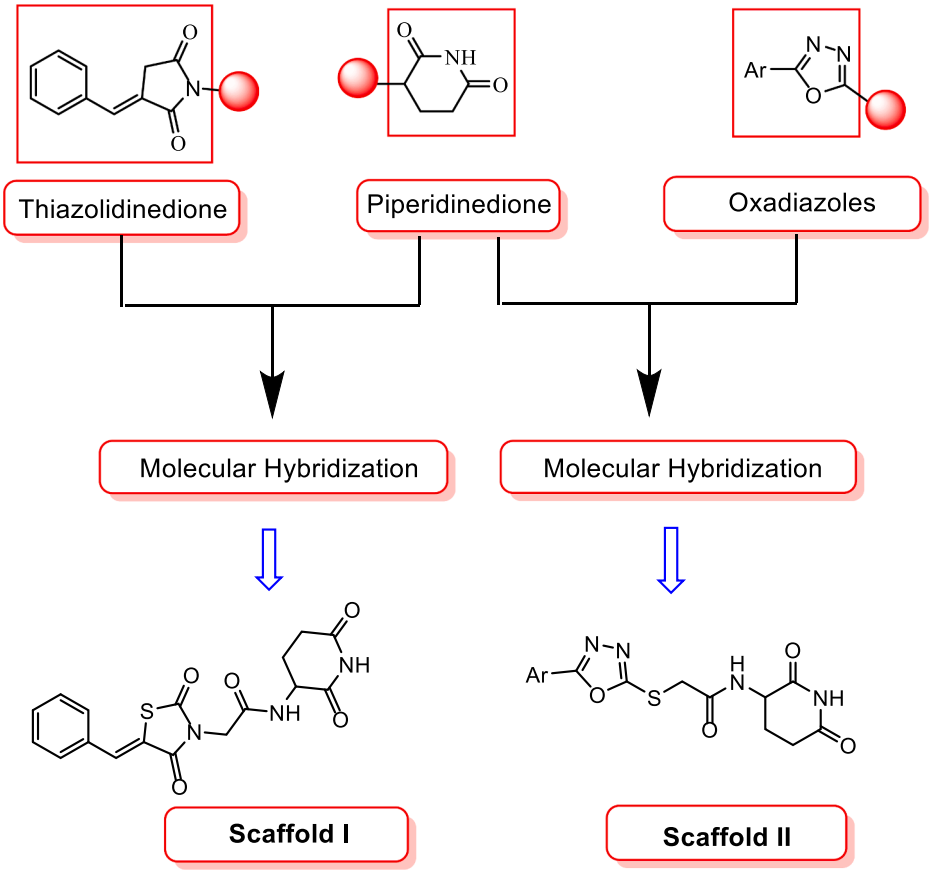

Fig. 3. Rationale concept to new thalidomide analogs.

from 28.13 ± 2.2 to 72.65 ± 4.6 μM against all cell lines. On the other hand, compounds **33$_c$, 33$_d$, 42$_{a-d}$** and **42$_g$** showed weak anti-proliferative activities against the tested cell. Finally, compounds **33$_b$, 33$_e$** and **33$_g$** were appeared to be inactive.

2.2.2. In vitro immunomodulatory assay

Four compounds **33$_h$, 33$_i$, 42$_f$** and **42$_h$** which exhibited cytotoxic activities higher than thalidomide against HCT-116 cancer cell line were selected and evaluated for their inhibitory effect on TNF-α and NF-κB *P*65 as well as their apoptotic and antiangiogenic activities. Thalidomide was used as a positive control in these procedures.

2.2.2.1. Estimation of human tumor necrosis factor alpha (TNF-α) in HCT-116 supernatant. In this test, the effect of the synthesized compounds **33$_h$, 33$_i$, 42$_f$** and **42$_h$** on **TNF-α** was examined. Thalidomide was used as a positive control. Two negative controls were used, the first one was untreated HCT-116 cells (control) and the second one was DMSO treated HCT-116 cells (control-DMSO).

The data presented in Fig. 6 showed that, production of TNF-α was significantly decreased in HCT-116 cells exposed to thalidomide and the synthesized compounds **33$_h$, 33$_i$, 42$_f$** and **42$_h$**, compared with control and control-DMSO cells. Comparing all the synthesized compounds with thalidomide revealed that compounds **33$_h$** and **42$_f$** showed

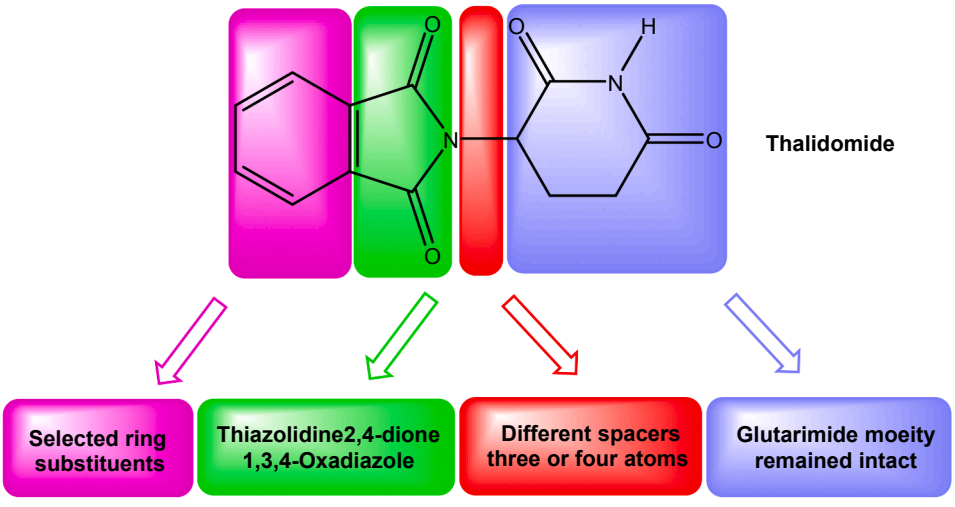

Fig. 4. Summary of structural modification modification of thalidomide.

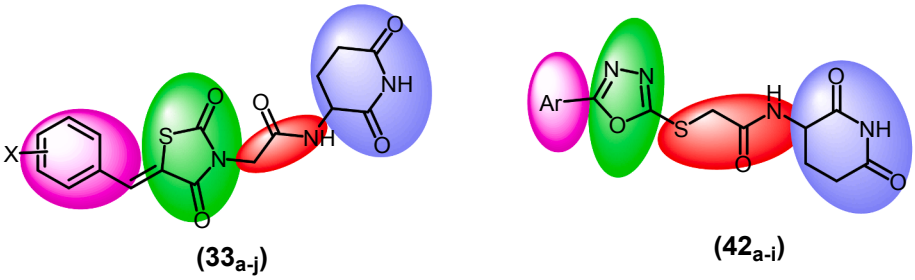

Fig. 5. New target compounds having the same essential pharmacophoric features of thalidomide.

remarkable significant reduction in TNF-α levels while compounds **33$_i$** and **42$_h$** represented insignificant increase in TNF-α levels in relation to thalidomide.

2.2.2.2. Estimation of human caspase-8 (CASP8) in HCT-116 supernatant. In this test, the effect of thalidomide and the synthesized compounds **33$_h$**, **33$_i$**, **42$_f$** and **42$_h$** on CASP8 was examined. As illustrated in Fig. 7, thalidomide and the synthesized compounds showed a statistically significant increase in CASP8 levels compared with control and control-DMSO cells. Comparing the tested compounds with thalidomide revealed that compounds **33$_i$** and **42$_f$** exhibited significant elevation in CASP8 levels. Furthermore, insignificant increase in CASP8 levels were presented after treatment with compounds **33$_h$** and **42$_h$** as compared with thalidomide.

2.2.2.3. Estimation of human vascular endothelial growth factor (VEGF) in HCT-116 supernatant. Assessment of the effect of thalidomide and the synthesized compounds **33$_h$**, **33$_i$**, **42$_f$** and **42$_h$** on **VEGF** was determined. The data in Fig. 8 indicated that, VEGF concentration was significantly decreased in HCT-116 cells after exposure to thalidomide and the synthesized compounds in comparison to the control and control-DMSO cells. Compounds **33$_i$** and **42$_f$** induced

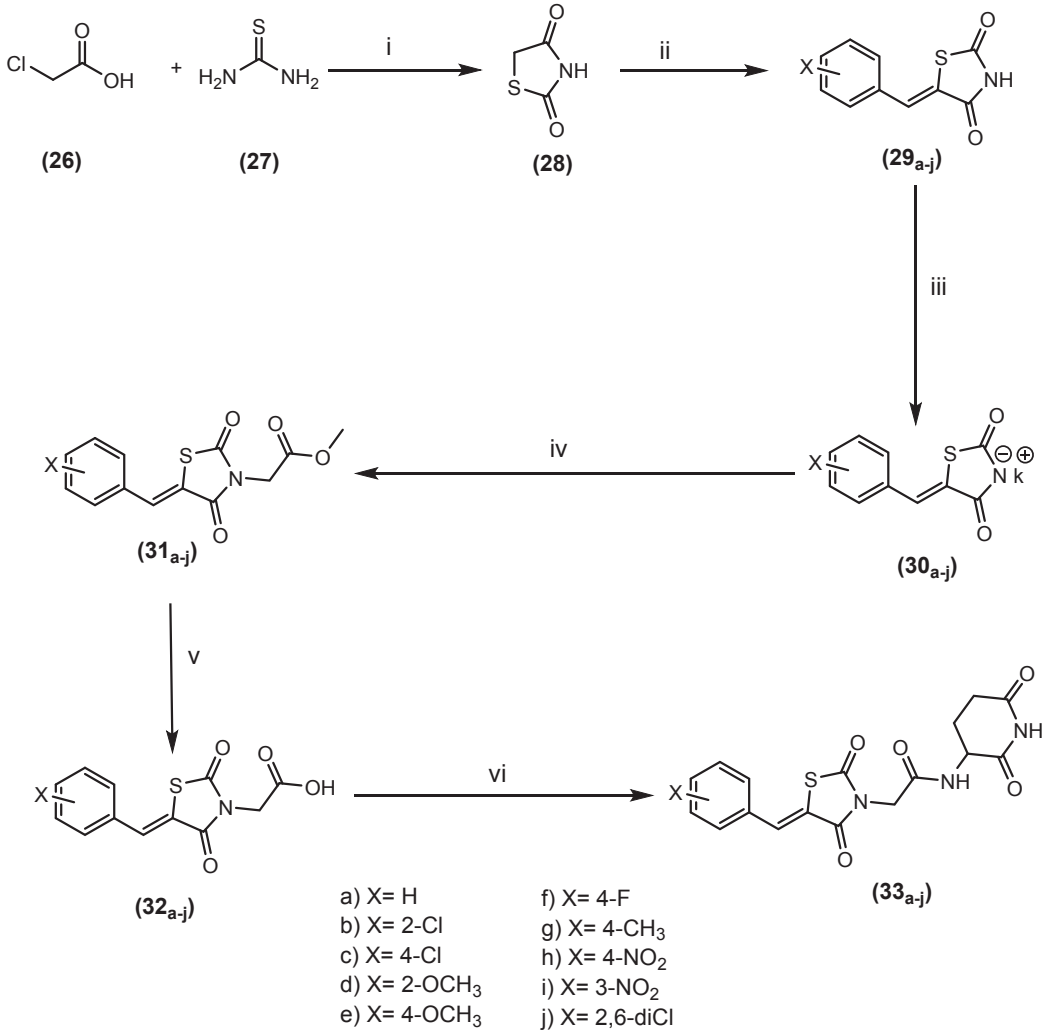

Scheme 1. General procedure for preparation of target compounds **33$_{a-j}$**; Reagents and conditions: (i) 4 N conc. HCl/reflux/10 h, (ii) absolute ethanol/piperidine/reflux/10 h, (iii) absolute ethanol/KOH/reflux, (iv) methyl bromoacetate/KI/Dry DMF/heating in water bath/4h, (v) glacial acetic acid/HCl/reflux/5h, (vi) TEA/ethyl chloroformate/30 min/TEA/3-aminopiperidine-2,6-dione HCl /r.t./12 h.

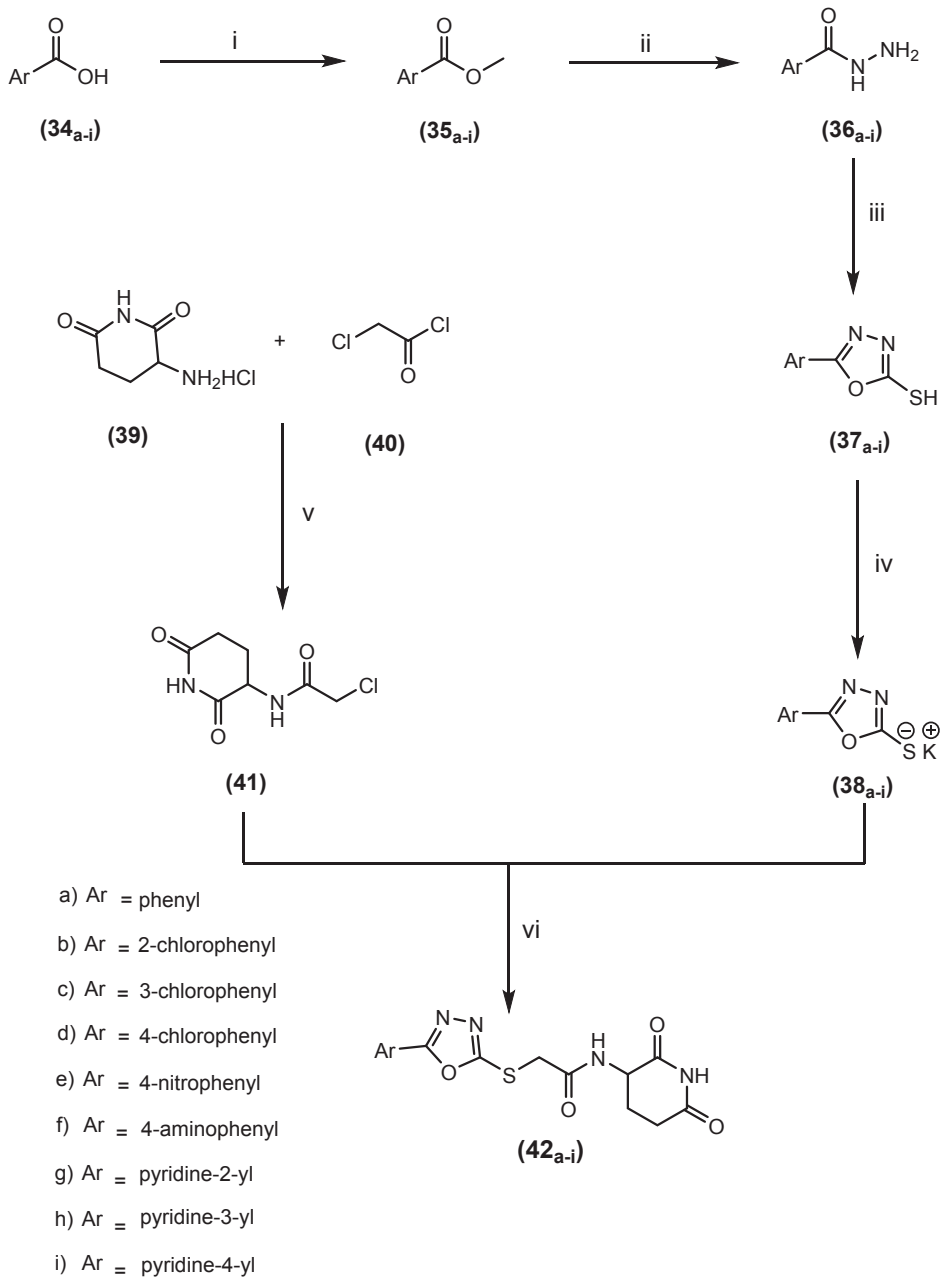

Scheme 2. General procedure for preparation of target compounds **42$_{a-i}$**; Reagents and conditions: (i) conc.H_2SO_4/methanol/reflux/5h, (ii) $NH_2NH_2{\cdot}H_2O$/absolute ethanol/reflux /6h, (iii) absolute ethanol/KOH/CS_2/reflux/6h, (iv) absolute ethanol/KOH/reflux, (v) $NaHCO_3$/DCM/H_2O, (vi) KI/acetonitrile/stirring at r.t./3h.

significantly lower levels of VEGF while compound **33$_h$** induced significantly higher level of VEGF in relation to thalidomide. In addition, compound **42$_h$** showed insignificant increase in VEGF level as compared to thalidomide.

2.2.2.4. Estimation of nuclear factor kappa-B P65 (NF-κB P65) in HCT-116 cell lysate. The effect of thalidomide and the synthesized compounds **33$_h$, 33$_i$, 42$_f$** and **42$_h$** on protein expression of NF-κB p65 was evaluated in the cell lysate.

According to the data in Fig. 9**,** there is a statistically significant decrease in NF-κB p65 levels after exposure of HCT-116 cells to thalidomide and the synthesized compounds. Comparing the synthesized compounds with thalidomide itself revealed that compound **42$_f$** showed significant decrease in level of NF-κB p65, in contrast, compounds **33$_h$** and **42$_h$** demonstrated a significant increase in levels of NF-κB p65. Compound **33$_i$** exhibited decrease in NF-κB p65 level although it's statistically insignificant.

2.2.3. Effect on cell cycle progression

Flow cytometric analysis technique [76] was used to examine the effect of compound **42$_f$** on cell cycle in HCT-116 cell line. The HCT-116 cells had been incubated for 24 h with 10 μM of compound **42$_f$.** Then**,** cell cycle parameters of incubated cells were compared with untreated control cells. The results revealed that HCT-116 cells accumulated at G2/M phase with percent of 40.52%. Moreover, the tested compound showed good ability to induce apoptosis at pre-G1 phase (Table 2, Figs. 10 and 12).

2.2.4. Induction of apoptosis

Annexin V/propidium iodide (PI) double staining assay method was

Table 1
Anti-proliferative activities of the target compounds against HepG-2, HCT-116, PC3 and MCF-7 cell lines.

Comp.	*In vitro* Cytotoxicity IC_{50} (μM)[a]			
	HepG-2	HCT-116	PC3	MCF-7
Thalidomide	61.10 ± 3.8	32.12 ± 3.2	76.91 ± 4.2	45.76 ± 3.6
33_a	42.35 ± 2.8	49.64 ± 3.9	69.34 ± 4.3	35.48 ± 2.7
33_b	NA[b]	90.78 ± 5.6	NA[b]	88.92 ± 5.5
33_c	67.22 ± 4.1	59.26 ± 4.5	76.01 ± 4.8	60.39 ± 3.9
33_d	79.12 ± 4.8	62.75 ± 4.6	83.81 ± 5.4	69.74 ± 4.5
33_e	NA[b]	82.68 ± 5.3	NA[b]	86.96 ± 5.4
33_f	63.04 ± 4.0	52.48 ± 4.1	72.65 ± 4.6	55.10 ± 3.7
33_g	NA[b]	NA[b]	NA[b]	NA[b]
33_h	21.34 ± 1.8	29.38 ± 2.8	42.96 ± 2.9	19.62 ± 1.6
33_i	23.96 ± 2.0	36.07 ± 3.2	49.90 ± 3.4	21.82 ± 1.8
33_j	31.75 ± 2.5	40.62 ± 3.4	55.78 ± 3.8	29.87 ± 2.1
42_a	69.92 ± 4.3	60.41 ± 4.6	78.36 ± 5.0	63.50 ± 4.1
42_b	65.58 ± 4.0	55.29 ± 4.4	74.50 ± 4.7	58.02 ± 3.9
42_c	56.70 ± 3.7	45.60 ± 3.6	61.38 ± 4.0	49.28 ± 3.5
42_d	91.26 ± 5.4	78.11 ± 5.0	94.56 ± 5.9	80.73 ± 4.9
42_e	28.13 ± 2.2	38.26 ± 3.3	52.23 ± 3.5	25.49 ± 1.9
42_f	16.48 ± 1.6	23.94 ± 2.3	28.43 ± 2.0	14.63 ± 1.3
42_g	81.84 ± 4.8	66.28 ± 4.8	85.44 ± 5.6	72.03 ± 4.7
42_h	19.47 ± 1.7	32.60 ± 2.9	46.81 ± 3.0	18.15 ± 1.5
42_i	37.62 ± 2.6	46.33 ± 3.7	65.82 ± 4.2	31.94 ± 2.4

[a] Three independent experiments were performed for each concentration.
[b] Compounds having IC_{50} value > 100 μM.

used to clarify the mechanism of induced cell death in HCT-116 cells at pre-G1 phase. HCT-116 cells were treated with 10 μM of the tested compound **42_f**. The results revealed that the percentage of total apoptosis induced by compound **42_f** was 21.34. In the early stage, there was significant increase in the percentage of apoptotic cells from 0.42% for control untreated cells up to 5.49%. Additionally, in the late phase, there was an increase in the apoptotic cells to attain 13.1% in comparison to 0.51% in control HCT-116 cells. The obtained results revealed that compound **42_f** induced pre-G1 apoptosis and arrested cell cycle at G2/M phase (Table 3 & Figs. 11 and 12).

3. Conclusion

In summary, nineteen derivatives of 3-aminopiperidine-2,6-dione derivatives have been designed and synthesized depending on thalidomide as a lead compound. Some derivatives exhibited anti-proliferative activities higher than thalidomide against HepG-2, HCT-116, PC3 and MCF-7 cell lines such as **33_h** (IC_{50} = 21.34 ± 1.8, 29.38 ± 2.8, 42.96 ± 2.9 and 19.62 ± 1.6 μM, respectively), **33_i** (IC_{50} = 23.96 ± 2.0, 36.07 ± 3.2, 49.90 ± 3.4 and 21.82 ± 1.8 μM, respectively), **42_f** (IC_{50} = 16.48 ± 1.6, 23.94 ± 2.3, 28.43 ± 2.0 and 14.63 ± 1.3 μM, respectively) and **42_h** (IC_{50} = 19.47 ± 1.7, 32.60 ± 2.9, 46.81 ± 3.0 and 18.15 ± 1.5 μM, respectively). Moreover, some compounds showed a significant reduction in TNF-α (compounds **33_h** and **42_f**), VEGF (compounds **33_i** and **42_f**) and NF-κB p65 (compounds **42_f**). Furthermore, some compounds exhibited significant elevation in CASP8 levels as compounds **33_i** and **42_f**). Additionally, Flow cytometry analysis demonstrated that compound **42_f** could significantly induce apoptosis (21.43%) of HCT-116 cells at a concentration of 10 μM and can arrest the cell cycle at G2/M phase. Structure-activity relationship study revealed that oxadiazole derivatives were more active than thiazolidine-2,4-dione ones. These results indicate that the designed compounds can act as promising immunomodulators and effective anticancer agents. Additionally, further optimization of these derivatives may result in discovering more promising immunomodulators.

4. Experimental

4.1. Chemistry

All melting points were performed by the open capillary method on a Gallen kamp device. The infrared spectra were verified using the potassium bromide disk technique on a pye Unicam SP 1000 IR spectrophotometer. Proton magnetic resonance ^{1}H NMR spectra and ^{13}C NMR spectra were recorded on a BRUKER 400 MHZ- NMR spectrometer. Chemical shifts were measured in δ scale (ppm) and TMS was used as internal standard. The mass spectra were recorded on Varian MAT 311-A (70 e.v.). Elemental analyses (C, H, N) of the tested compounds were carried out on a CHN analyzer. All compounds were within ± 0.4 of the theoretical values. The reactions were monitored by thin-layer chromatography (TLC) using TLC sheets precoated with UV fluorescent silica gel Merck 60 F254 plates and were envisaged using UV lamp and different solvents as mobile phases. Compounds **28, 29_{a-j}, 30 $_{a-j}$, 31 $_{a-j}$, 32_{a-j}, 35_{a-i}, 36_{a-i}, 37_{a-i}**, and **38_{a-i}** were synthesized according to reported methods [65,66,73,74,77]

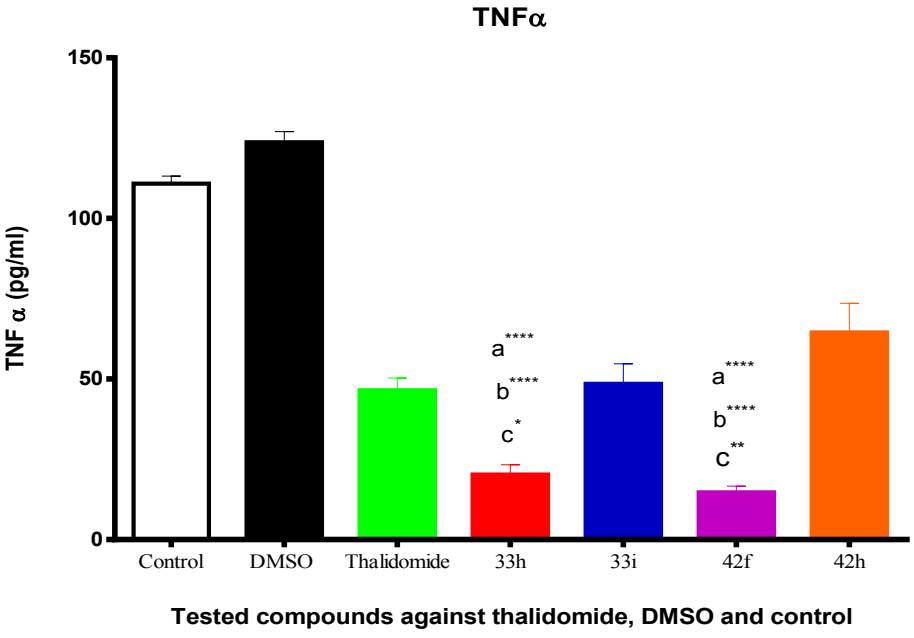

Fig. 6. Levels of TNF α in the cell supernatant after exposure to 10 μM of thalidomide and the synthesized compounds on HCT-116 cells. (a) Denotes group statistically significant from control cells, (b) Denotes group statistically significant from control-DMSO cells, (c) Denotes group statistically significant from thalidomide. Results are expressed as mean ± SEM. *(P < 0.05), **(P < 0.01),***(P < 0.001).

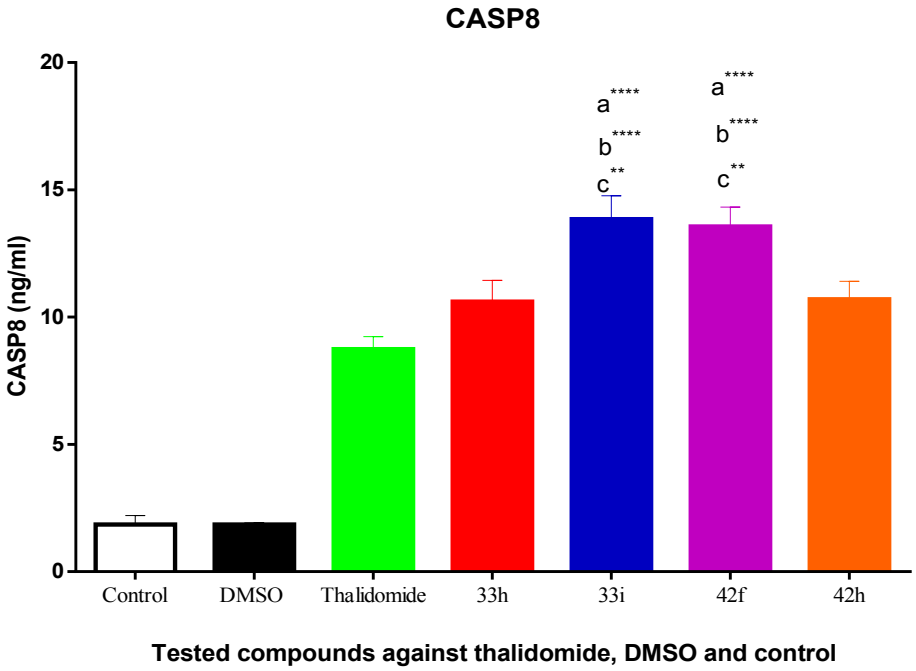

Fig. 7. Levels of CASP8 in the cell supernatant after exposure to 10 μM of thalidomide and the synthesized compounds on HCT-116 cells. (a) Denotes group statistically significant from control cells, (b) Denotes group statistically significant from control-DMSO cells, (c) Denotes group statistically significant from thalidomide. Results are expressed as mean ± SEM. *(P < 0.05), **(P < 0.01),***(P < 0.001).

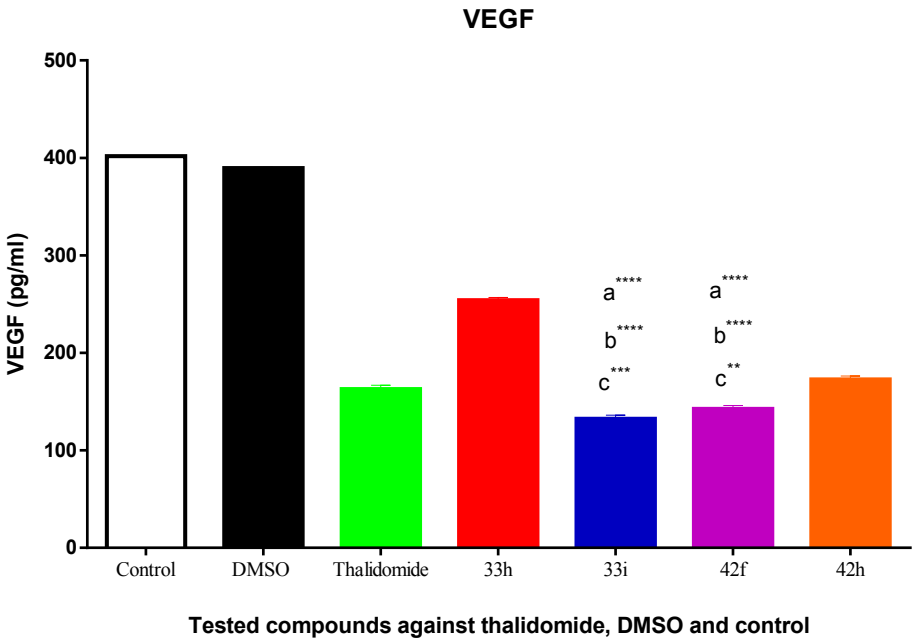

Fig. 8. Levels of VEGF in the cell supernatant after exposure to 10 μM of thalidomide and the synthesized compounds on HCT-116 cells. (a) Denotes group statistically significant from control cells, (b) Denotes group statistically significant from control DMSO cells, (c) Denotes group statistically significant from thalidomide. Results are expressed as mean ± SEM. *(P < 0.05), **(P < 0.01),***(P < 0.001).

4.1.1. General procedure for synthesis of compounds (11_{a-j})

To a suspension of the appropriate acid $\mathbf{32_{a-j}}$ (3 mmol) in DCM (10 mL), Et3N (0.33 g, 0.46 mL, 3.30 mmol) was added. The reaction mixture was stirred in ice-salt bath for 10 min. To the previous clear solution, ethyl chloroformate (0.35 g, 0.31 mL, 3.30 mmol) was added in a drop wise manner over a period of 20 min. and the reaction mixture was stirred for 1 h in the ice-salt bath. A solution of 3-aminopiperidine-2,6-dione HCl (0.49 g, 3 mmol) and Et3N (0.33 g, 0.46 mL, 3.30 mmol) in DCM (10 mL) was added to the reaction mixture. The whole mixture was allowed to stir for 12 h at r.t. and the obtained precipitates were filtered, washed with water followed by hot DCM and dried to furnish the corresponding target compounds $\mathbf{33_{a-j}}$, respectively.

4.1.1.1. 2-(5-Benzylidene-2,4-dioxothiazolidin-3-yl)-N-(2,6-dioxopiperidin-3-yl) acetamide (33_a). White crystal (yield, 75%); m.p. = 266–268 °C. IR (KBr, cm^{-1}): 3360, 3225 (NH), 3134 (CH aromatic), 2972 (CH aliphatic) and 1692 (C═O amide); ^{1}H NMR (DMSO-d_6) δ ppm: 1.91–1.97 (m, 2H, $\mathbf{CH_2}$CH of piperidine), 2.48–2.52 (m, 1H, CH_2CO of piperidine), 2.68–2.75 (m, 1H, CH_2CO of piperidine), 4.36 (s, 2H, $\mathbf{CH_2}$CONH), 4.40–4.62 (m, 1H, CH of piperidine), 7.49–7.53 (dd, 1H, C-4 phenyl, J = 8.4 *Hz* & 8.2 *Hz*), 7.54–7.58 (dd, 2H, C-3 and C-5 phenyl, J = 8.4 *Hz* & 8 *Hz*), 7.64–7.66 (d, 2H, C-2 and C-6 phenyl, J = 8 *Hz*), 7.98 (s, 1H, −C═CH), 7.72–7.74 (d, 1H, J = 8.1 *Hz*, NHCO, D_2O exchangeable), 10.87 (s, 1H, CONHCO, D_2O exchangeable); ^{13}C NMR (DMSO-d_6, 100 MHz) δ (ppm): 24.71, 31.25, 43.85, 49.90, 121.58, 129.90(2C), 130.64(2C), 131.25, 133.35, 133.88, 165.61, 165.70, 167.51, 172.19, 173.32; Anal. Calcd. for $C_{17}H_{15}N_3O_5S$ (373.38): C, 54.69; H, 4.05; N, 11.25. Found: C, 54.30; H, 4.09; N, 11.51%.

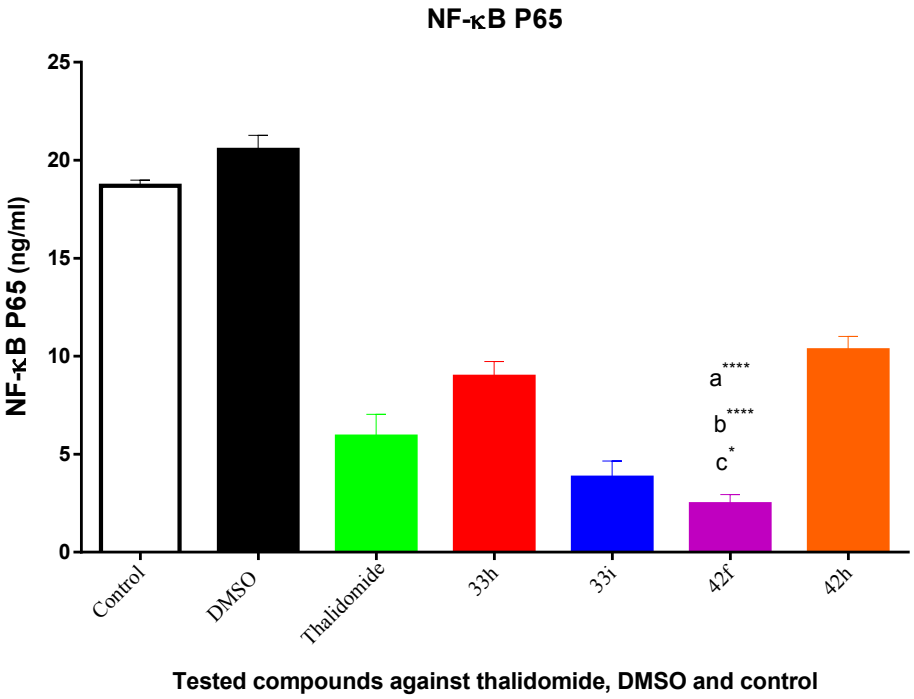

Fig. 9. Levels of NF-κB p65 in the cell lysate after exposure to 10 μM of thalidomide analogs on HCT-116 cells. (a) Denotes group statistically significant from control cells, (b) Denotes group statistically significant from control DMSO cells, (c) Denotes group statistically significant from thalidomide. Results are expressed as mean ± SEM. *($P < 0.05$), **($P < 0.01$),***($P < 0.001$).

Table 2
Effect of compound **42$_f$** on cell cycle progression in HCT-116 cells.

Sample	Cell cycle distribution (%)			
	%G0/G1	%S	%G2/M	%Pre-G1
42$_f$/HCT-116 cell	41.29	18.19	40.52	21.34
Cont. HCT-116 cell	57.41	26.84	15.75	2.19

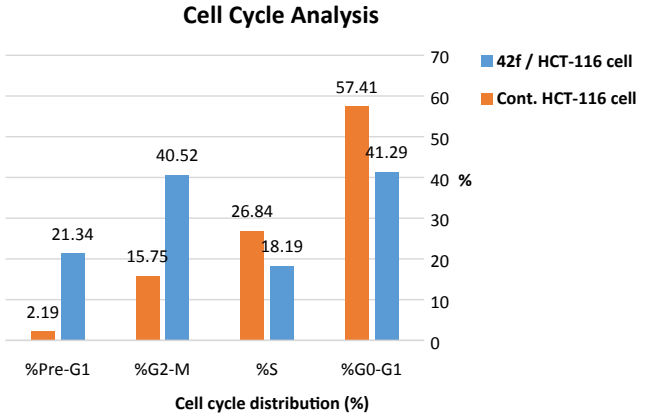

Fig. 10. Cell cycle analysis and apoptosis effect in HCT-116 cell line when treated with compound **42$_f$**.

Table 3
Apoptosis and necrosis percent induced by compound **42$_f$** on HCT-116 cells.

Sample	Apoptosis			Necrosis
	Total	Early	Late	
42$_f$/HCT-116	21.34	5.49	13.1	2.75
Cont. HCT-116	2.19	0.42	0.51	1.26

*4.1.1.2. 2-(5-(2-Chlorobenzylidene)-2,4-dioxothiazolidin-3-yl)-N-(2,6 dioxopiperidin-3-yl)acetamide (**33$_b$**).* Grayish white crystal (yield, 67%); m.p. = 245–247 °C. IR (KBr, cm^{-1}): 3346, 3249 (NH), 3135 (CH aromatic), 2990 (CH aliphatic) and 1695 (C=O amide); ^{1}H NMR (DMSO-d_6) δ ppm: 1.88–1.97 (m, 2H, **CH$_2$**CH of piperidine), 2.50–2.54 (m, 1H, CH$_2$CO of piperidine), 2.68–2.78 (m, 1H, CH$_2$CO of piperidine), 4.37 (s, 2H, CH$_2$CONH), 4.56–4.62 (m, 1H, CH of piperidine), 7.53–7.55 (dd, 1H, C-4 phenyl), 7.61–7.65 (m, 2H, C-5 and C-6 phenyl), 7.65–7.67 (d, 1H, C-3 phenyl), 8.06 (s, 1H, −C=CH), 8.72–8.74 (d, 1H, J = 7.9 Hz, NHCO, D$_2$O exchangeable), 10.88 (s, 1H, CONHCO, D$_2$O exchangeable); MS (*m/z*): 409 (M^+ + 2, 4.58%), 407 (M^+, 17.92%), 372 (100%, base peak); Anal. Calcd. for $C_{17}H_{14}ClN_3O_5S$ (407.83): C, 50.07; H, 3.46; N, 10.30. Found: C, 50.10; H, 3.26; N, 10.22%.

*4.1.1.3. 2-(5-(4-Chlorobenzylidene)-2,4-dioxothiazolidin-3-yl)-N-(2,6-dioxopiperidin-3-yl)acetamide (**33$_c$**).* White crystal (yield, 75%); m.p. = 256–258 °C. IR (KBr, cm^{-1}): 3431, 3284 (NH), 3102 (C−H aromatic), 2907 (C−H aliphatic) and 1690 (C=O amide); ^{1}H NMR (DMSO-d_6) δ ppm: 1.93–1.97 (m, 2H, **CH$_2$**CH of piperidine), 2.50–2.51 (m, 1H, **CH$_2$**CO of piperidine), 2.70–2.74 (m, 1H, **CH$_2$**CO of piperidine), 4.36 (s, 2H, **CH$_2$**CONH), 4.55–4.62 (m, 1H, **CH** piperidine), 7.61–7.63 (d, 2H, C-3 and C-5 phenyl, J = 8 *Hz*), 7.67–7.69 (d, 2H, C-2 and C-6 phenyl, J = 8 *Hz*), 7.98 (s, 1H, −C=CH), 8.70–8.72 (d, 1H, J = 8.1 *Hz*, NHCO, D$_2$O exchangeable), 10.86 (s, 1H, CONHCO, D$_2$O exchangeable); Anal. Calcd. for $C_{17}H_{14}ClN_3O_5S$ (407.83): C, 50.07; H, 3.46; N, 10.30. Found: C, 50.25; H, 3.12; N, 10.24%.

*4.1.1.4. N-(2,6-Dioxopiperidin-3-yl)-2-(5-(2-methoxybenzylidene)-2,4-dioxothiazolidin-3-yl)acetamide (**33$_d$**).* Yellow crystal (yield, 69%); m.p. = 272–274 °C. IR (KBr, cm^{-1}): 3311, 3202 (2NH), 3090 (C−H aromatic), 2935 (C−H aliphatic) and 1693 (C=O amide); ^{1}H NMR (DMSO-d_6) δ ppm: 1.94–1.97 (m, 2H, **CH$_2$**CH of piperidine), 2.50–2.51 (m, 1H, **CH$_2$**CO of piperidine), 2.68–2.78 (m, 1H, **CH$_2$**CO of piperidine), 3.90 (s, 3H, O**CH$_3$**), 4.35 (s, 2H, **CH$_2$**CO), 4.55–4.62 (m, 1H, **CH**CO), 7.10–7.14 (dd, 1H, C-5 phenyl, J = 8.1 *Hz* & 7.6 *Hz*), 7.17–7.19 (d, 1H, J = 8.4 *Hz*, C-3 phenyl), 7.46–7.48 (d, 1H, C-6 phenyl, J = 8.1 Hz), 7.50–7.54 (dd, 1H, C-4 phenyl, J = 8.3 &7.1 Hz), 8.10 (s, 1H, −C=CH), 8.70–8.72 (d, 1H, J = 8.1 Hz, NHCO, D$_2$O exchangeable), 10.89 (s, 1H,

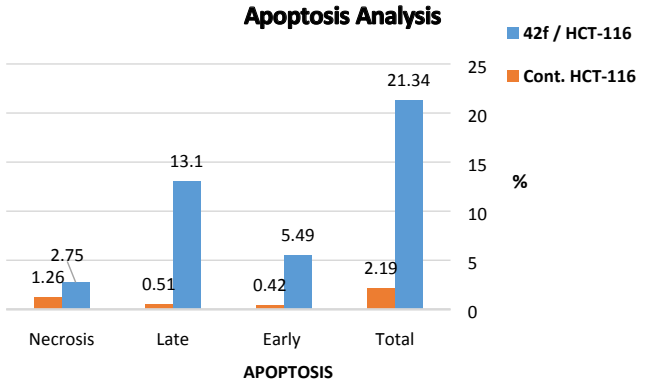

Fig. 11. Percentage of induced cell death by compound **42$_f$** on HCT-116 cells.

CONHCO, D_2O exchangeable); MS (*m/z*): 391 (M^+, 61.85%), 151 (100%, base peak); Anal. Calcd. for $C_{18}H_{17}N_3O_6S$ (403.41): C, 53.59; H, 4.25; N, 10.42. Found: C, 53.81; H, 4.09; N, 10.19%.

*4.1.1.5. N-(2,6-Dioxopiperidin-3-yl)-2-(5-(4-methoxybenzylidene)-2,4-dioxothiazolidin-3-yl)acetamide (**33$_e$**).* Yellowish white crystal (yield, 76%); m.p. = 276–278 °C. IR (KBr, cm^{-1}): 3413, 3287 (NH), 3101 (C—H aromatic), 2926 (C—H aliphatic) and 1687 (C═O amide); ^{1}H NMR (DMSO-d_6) δ ppm: 1.94–1.96 (m, 2H, **CH$_2$**CH of piperidine), 2.48–2.53 (m, 1H, **CH$_2$**CO of piperidine), 2.68–2.77 (m, 1H, **CH$_2$**CO of piperidine), 3.83 (s, 3H, O**CH$_3$**), 4.35 (s, 2H, **CH$_2$**CO), 4.55–4.61 (m, 1H, **CH**CO), 7.10–7.12 (d, 2H, C-3 and C-5 phenyl, *J* = 8.1 Hz), 7.60–7.62 (d, 2H, C-2 and C-6 phenyl, *J* = 7.8 Hz), 7.91 (s, 1H, —C═CH), 8.70–8.72 (d, 1H, *J* = 8.2 Hz, NHCO, D_2O exchangeable), 10.87 (s, 1H, CONHCO, D_2O exchangeable); ^{13}C NMR (DMSO-d_6, 100 MHz) δ (ppm): 21.59, 24.71, 31.24, 43.81, 49.89, 120.33, 130.52(2C), 130.60(2C), 130.72, 133.94, 141.63, 165.64, 165.76, 167.54, 172.18, 173.32; Anal. Calcd. for $C_{18}H_{17}N_3O_6S$ (403.41): C, 53.59; H, 4.25; N, 10.42. Found: C, 53.48; H, 4.32; N, 10.51%.

*4.1.1.6. N-(2,6-Dioxopiperidin-3-yl)-2-(5-(4-fluorobenzylidene)-2,4-dioxothiazolidin-3-yl)acetamide (**33$_f$**).* White crystal (yield, 74%); m.p. = 235–237 °C. IR (KBr, cm^{-1}): 3289 (2NH), 3091 (C—H aromatic), 2890 (C—H aliphatic) and 1688 (C═O amide); ^{1}H NMR (DMSO-d_6) δ ppm: 1.91–1.97 (m, 2H, **CH$_2$**CH of piperidine), 2.48–2.52 (m, 1H, CH_2CO of piperidine), 2.69–2.78 (m, 1H, CH_2CO of piperidine), 4.35 (s, 2H, CH_2CONH), 4.55–4.62 (m, 1H, CH piperidine), 7.38–7.42 (d, 2H, *J* = 8 Hz, C-3 and C-5 phenyl), 7.71–7.75 (d, 2H, *J* = 8 Hz, C-2 and C-6 phenyl), 7.99 (s, 1H, —C═CH), 8.71–8.73 (d, 1H, *J* = 8.2 *Hz*, NHCO, D_2O exchangeable), 10.87 (s, 1H, CONHCO, D_2O exchangeable); MS (*m/z*): 391 (M^+, 61.85%), 151 (100%, base peak); Anal. Calcd. for $C_{17}H_{14}FN_3O_5S$ (391.37): C, 52.17; H, 3.61; N, 10.74. Found: C, 52.33; H, 3.35; N, 10.49%.

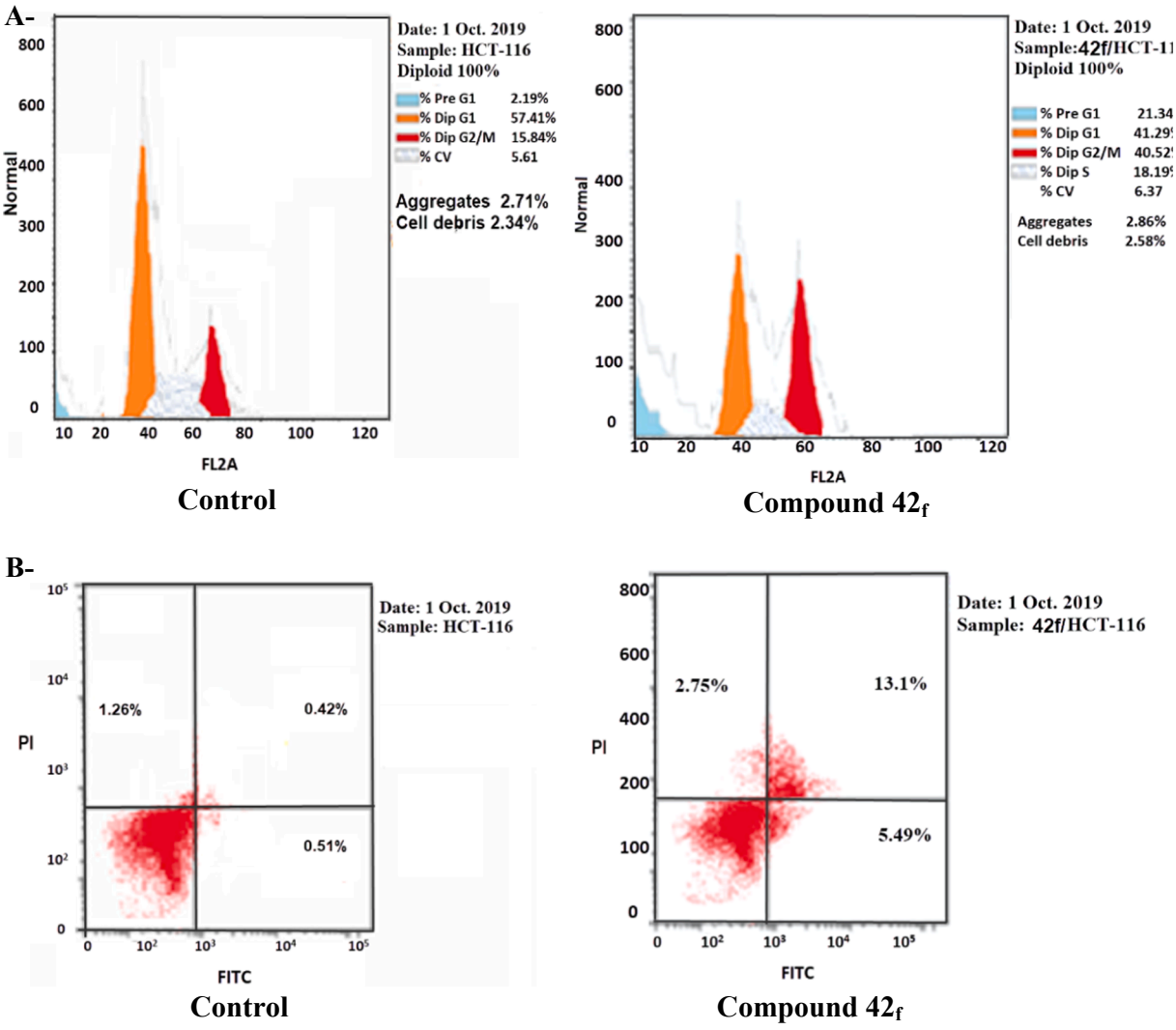

Fig. 12. A) HCT-116 cells distribution upon treatment with compound **42$_f$**. **B)** Induced apoptosis on HCT-116 cells by compound **42$_f$**.

*4.1.1.7. N-(2,6-Dioxopiperidin-3-yl)-2-(5-(4-methylbenzylidene)-2,4-dioxothiazolidin-3-yl)acetamide (**33$_g$**).* Off white crystal (yield, 68%); m.p. = 230–232 °C. IR (KBr, cm^{-1}): 3291, 3251 (2NH), 3105 (C—H aromatic), 2950 (C—H aliphatic) and 1688 (C=O amide); ^{1}H NMR (DMSO-d_6) δ ppm: 1.94–1.95 (m, 2H, **CH$_2$**CH of piperidine), 2.37 (s, 3H, CH_3), 2.48–2.51 (m, 1H, CH_2CO of piperidine), 2.68–2.76 (m, 1H, CH_2CO of piperidine), 4.35 (m, 2H, **CH$_2$**CONH), 4.55–4.61 (m, 1H, CH of piperidine), 7.37–7.39 (d, 2H, C-3 and C-5 phenyl, J = 7.8 Hz), 7.54–7.56 (d, 2H, C-2 and C-6 phenyl, J = 8.2 Hz), 7.93 (s, 1H, —C=CH), 8.72–8.74 (d, 1H, J = 8 Hz, NHCO, D_2O exchangeable), 10.87 (s, 1H, CONHCO, D_2O exchangeable); ^{13}C NMR (DMSO-d_6, 100 MHz) δ (ppm): 24.72, 31.25, 43.77, 49.90, 56.00, 115.49(2C), 118.24, 125.81, 132.80(2C), 133.88, 161.75, 165.69, 165.82, 167.59, 172.20, 173.33; Anal. Calcd. for $C_{18}H_{17}N_3O_5S$ (387.41): C, 55.81; H, 4.42; N, 10.85. Found: C, 55.61; H, 4.63; N, 10.56%.

*4.1.1.8. N-(2,6-Dioxopiperidin-3-yl)-2-(5-(4-nitrobenzylidene)-2,4-dioxothiazolidin-3-yl)acetamide (**33$_h$**).* Shine yellow crystal (yield, 72%); m.p. = 240–242 °**C**. IR (KBr, cm^{-1}): 3432, 3291 (NH), 3098 (C—H aromatic), 2938 (C—H aliphatic) and 1695 (C=O amide); ^{1}H NMR (DMSO-d_6) δ ppm: 1.91–1.96 (m, 2H, **CH$_2$**CH of piperidine), 2.50–2.52 (m, 1H, **CH$_2$**CO of piperidine), 2.69–2.76 (m, 1H, **CH$_2$**CO of piperidine), 4.33–4.42 (m, 2H, **CH$_2$**CO), 4.53–4.62 (m, 1H, **CH**CO), 7.91–7.93 (d, 2H, C-2 and C-6 phenyl, J = 8.2 Hz), 8.09 (s, 1H, —C=**CH**), 8.36–8.37 (d, 2H, C-3 and C-5 phenyl, J = 7.5 Hz), 8.72–8.75 (d, 1H, J = 12 Hz, **NH**CO, D_2O exchangeable), 10.87 (s, 1H, CO**NH**CO, D_2O exchangeable); MS (*m/z*): 418 (M^+, 95.58%), 55 (100%, base peak), 366 (53.41%), 290 (48.51%), 236 (53.42%), 178 (71.86%), 160 (48.74%), 120 (49.45%), 82 (54.04%); Anal. Calcd. for $C_{17}H_{14}N_4O_7S$ (418.38): C, 48.80; H, 3.37; N, 13.39. Found: C, 48.44; H, 3.00; N, 13.57%.

*4.1.1.9. N-(2,6-Dioxopiperidin-3-yl)-2-(5-(3-nitrobenzylidene)-2,4-dioxothiazolidin-3-yl)acetamide (**33$_i$**).* Yellow crystal (yield, 75%); m.p. = 228–230 °C. IR (KBr, cm^{-1}): 3292, 3248 (2NH), 3130 (C—H aromatic), 3095 (C—H aliphatic) and 1696 (C=O amide); ^{1}H NMR (DMSO-d_6) δ ppm: 1.88–1.95 (m, 2H, **CH$_2$**CH of piperidine), 2.48–2.52 (m, 1H, **CH$_2$**CO of piperidine), 2.69–2.77 (m, 1H, **CH$_2$**CO of piperidine), 4.38 (s, 2H, **CH$_2$**CO), 4.53–4.66 (m, 1H, **CH**CO), 7.83–7.87 (dd, 1H, C-5 phenyl, J = 8.2 *Hz* & 7.1 Hz), 8.06–8.07 (d, 1H, C-6 phenyl, J = 8.2 Hz), 8.15 (s, 1H, —C=**CH**), 8.31–8.33 (d, 1H, C-4 phenyl, J = 7.1 Hz), 8.51 (s, 1H, C-3 phenyl), 8.72–8.74 (d, 1H, J = 8.1 Hz, **NH**CO, D_2O exchangeable), 10.87 (s, 1H, CO**NH**CO, D_2O exchangeable); Anal. Calcd. for $C_{17}H_{14}N_4O_7S$ (418.38): C, 48.80; H, 3.37; N, 13.39. Found: C, 48.64; H, 3.48; N, 13.53%

*4.1.1.10. 2-(5-(2,6-Dichlorobenzylidene)-2,4-dioxothiazolidin-3-yl)-N-(2,6-dioxopipe- ridin-3-yl)acetamide (**33$_j$**).* White crystal (yield, 71%); m.p. = 263–265 °**C**. IR (KBr, cm^{-1}): 3353, 3242 (2NH), 3095 (C—H aromatic), 2976 (C—H aliphatic) and 1699 (C=O amide); ^{1}H NMR (DMSO-d_6) δ ppm: 1.93–1.97 (m, 2H, **CH$_2$**CH of piperidine), 2.50–2.53 (m, 1H, **CH$_2$**CO of piperidine), 2.63–2.77 (m, 1H, **CH$_2$**CO of piperidine), 4.36 (s, 2H, **CH$_2$**CO), 4.37–4.61 (m, 1H, **CH**CO), 7.50–7.54 (dd, 1H, C-4 phenyl, J = 8.0 Hz & 7.8 Hz), 7.62–7.64 (d, 2H, C-3 and C-5 phenyl, J = 8.0 Hz), 7.91 (s, 1H, —C=**CH**), 8.76–8.78 (d, 1H, J = 8 Hz, **NH**CO, D_2O exchangeable), 10.87 (s, 1H, CO**NH**CO, D_2O exchangeable); MS (*m/z*): 442 (M^+, 6.69%), 55 (100%, base peak), 405 (54.23%), 203 (32.26%), 166 (21.93%), 131 (20.87%), 122 (19.78%), 83 (44.55%). Anal. Calcd. for $C_{17}H_{13}Cl_2N_3O_5S$ (442.27): C, 46.17; H, 2.96; N, 9.50. Found: C, 46.41; H, 3.19; N, 9.72%.

*4.1.2. 2-Chloro-N-(2,6-dioxopiperidin-3-yl)acetamide (**41**)*

A mixture of 3-aminopiperidine-2,6-dione HCl (3 g, 18.23 mmol) and $NaHCO_3$ (3.06 g, 36.45 mmol) was dissolved in water (20 mL) while stirring until complete dissolution. DCM (10 mL) was added to the aqueous solution in an ice bath. A solution of chloroacetyl chloride (2.26 g, 1.59 mL, 20.05 mmol) in DCM (10 mL) was added drop wise to the previous solution over a period of 0.5 h while stirring in the ice bath. The reaction mixture was allowed to stir at r.t. for an extra 0.5 h. The obtained precipitate was filtered, washed with DCM and dried to afford a white product. The filtrate was extracted with ethyl acetate (10 mL × 3), dried over $MgSO_4$ anhydrous and filtered. Upon concentration of ethyl acetate a second crop of white product was obtained to give compound **41**.

Shine white crystal (yield, 80%); m.p. = 148–150 °**C**. IR (KBr, cm^{-1}): 3316, 3189 (2NH), 2871 (C—H aliphatic), 1708 (C=O imide), 1659 (C=O amide); ^{1}H NMR (DMSO-d_6) δ ppm: 1.92–1.97 (m, 2H, **CH$_2$**CH of piperidine), 2.50–2.51 (m, 1H, **CH$_2$**CO of piperidine), 2.72–2.80 (m, 1H, **CH$_2$**CO of piperidine), 4.16 (s, 2H, Cl**CH$_2$**CO), 4.56–4.63 (m, 1H, **CH**CO), 8.57 (d, 1H, J = 8.0 Hz, **NH**CO), 10.86 (s, 1H, CO**NH**CO).

*4.1.3. General procedure for synthesis of compounds (**42$_{a\text{-}i}$**)*

A mixture of the appropriate potassium salt of 5-un(substituted) aryl-1,3,4-oxadiazole-2-thiol **(17$_{a\text{-}i}$)** (2 mmol) and 2-chloro-*N*-(2,6-dioxopiperidin-3-yl)acetamide **(42)** (0.49 g, 2.40 mmol) in the presence of catalytic amount of potassium iodide in acetonitrile (20 mL) was stirred at r.t. for 12 h. The obtained precipitates were filtered off, washed with water, dried and crystallized from methanol to afford the corresponding acetamide derivatives **(42$_{a\text{-}i}$)** respectively.

*4.1.3.1. N-(2,6-Dioxopiperidin-3-yl)-2-[(5-phenyl-1,3,4-oxadiazol-2-yl) thio]acetamide (**42$_a$**).* Off white crystal (yield, 85%); m.p. = 185–187 °**C**. IR (KBr, cm^{-1}): 3288, 3198 (NH), 3097 (C—H aromatic), 2878 (C—H aliphatic), 1708 (C=O imide) and 1676 (C=O amide); ^{1}H NMR (DMSO-d_6) δ ppm: 1.94–1.97 (m, 2H, **CH$_2$**CH of piperidine), 2.48–2.51 (m, 1H, **CH$_2$**CO of piperidine), 2.68–2.78 (m, 1H, **CH$_2$**CO of piperidine), 4.20 (s, 2H, **CH$_2$**CO), 4.58–4.64 (m, 1H, **CH**CO), 7.59–7.61 (m, 3H, Ar-H), 7.97–7.99 (d, 2H, C-2 and C-6 phenyl, J = 8 Hz), 8.72–8.75 (d, 1H, J = 12 Hz, **NH**CO, D_2O exchangeable), 10.86 (s, 1H, CO**NH**CO, D_2O exchangeable); ^{13}C NMR (DMSO-d_6, 100 MHz) δ (ppm): 24.60, 31.26, 36.04, 50.15, 123.50, 126.88(2C), 129.88(2C), 132.47, 163.72, 165.57, 166.68, 172.20, 173.30; Anal. Calcd. for $C_{15}H_{14}N_4O_4S$ (346.36): C, 52.02; H, 4.07; N, 16.18. Found: C, 52.41; H, 4.35; N, 16.38%

*4.1.3.2. 2-[(5-(2-Chlorophenyl)-1,3,4-oxadiazol-2-yl)thio]-N-(2,6-dioxopiperidin-3-yl)acetamide (**42$_b$**).* White crystal (yield, 82%); m.p. = 198–200 °**C**. IR (KBr, cm^{-1}): 3291 (br, 2NH), 3101 (C—H aromatic), 2925, 2876 (C—H aliphatic), 1711 (C=O imide) and 1668 (C=O amide); ^{1}H NMR (DMSO-d_6) δ ppm: 1.95–1.97 (m, 2H, **CH$_2$**CH of piperidine), 2.47–2.50 (m, 1H, **CH$_2$**CO of piperidine), 2.69–2.77 (m, 1H, **CH$_2$**CO of piperidine), 4.21 (s, 2H, **CH$_2$**CO), 4.57–4.63 (m, 1H, **CH**CO), 7.60–7.64 (dd, 1H, J = 8.2 Hz & 7.8 Hz, C-4 phenyl), 7.70–7.74 (dd, 1H, J = 8.2 & 8.0 Hz, C-5 phenyl), 7.94–7.96 (d, 1H, J = 7.8 Hz, C-3 phenyl), 7.96–7.98 (d, 1H, J = 8.0 Hz, C-6 phenyl), 8.74–8.75 (d, 1H, J = 4 Hz, **NH**CO, D_2O exchangeable), 10.85 (s, 1H, CO**NH**CO, D_2O exchangeable); MS (*m/z*): 379 (M^+, 26.04%), 111 (100%, base peak), 141 (92.13%), 271 (27.06%), 378 (21.31%), 75 (22.93%); Anal. Calcd. for $C_{15}H_{13}ClN_4O_4S$ (380.80): C, 47.31; H, 3.44; N, 14.71. Found: C, 47.52; H, 3.62; N, 14.45%.

*4.1.3.3. 2-[(5-(3-Chlorophenyl)-1,3,4-oxadiazol-2-yl)thio]-N-(2,6-dioxopiperidin-3-yl)acetamide (**42$_c$**).* Grayish white crystal (yield, 85%); m.p. = 224–226 °**C**. IR (KBr, cm^{-1}): 3289, 3199 (2NH), 3099 (C—H aromatic), 2922, 2865 (C—H aliphatic), 1708 (C=O imide) and 1669 (C=O amide); ^{1}H NMR (DMSO-d_6) δ ppm: 1.92–1.97 (m, 2H, **CH$_2$**CH of piperidine), 2.49–2.51 (m, 1H, **CH$_2$**CO of piperidine), 2.68–2.71 (m, 1H, **CH$_2$**CO of piperidine), 4.19 (s, 2H, **CH$_2$**CO), 4.59–4.63 (m, 1H, **CH**CO), 7.66–7.68 (d, 1H, C-5 phenyl, J = 8.2 Hz), 7.70–7.72 (dd, 1H, C-4 phenyl, J = 8.2 & 7.8 Hz), 7.76–7.78 (d, 1H, C-6 phenyl, J = 8.2 Hz), 7.95 (s, 1H, C-2 phenyl), 8.71–8.73 (d, 1H, J = 8.0 Hz,

NHCO, D_2O exchangeable), 10.85 (s, 1H, CO**NH**CO, D_2O exchangeable); Anal. Calcd. for $C_{15}H_{13}ClN_4O_4S$ (380.80): C, 47.31; H, 3.44; N, 14.71. Found: C, 47.11; H, 3.22; N, 14.53%.

*4.1.3.4. 2-[(5-(4-Chlorophenyl)-1,3,4-oxadiazol-2-yl)thio]-N-(2,6-dioxopiperidin-3-yl)acetamide (**42$_d$**).* Off white crystal (yield, 89%); m.p. = 234–236 °**C**. IR (KBr, cm^{-1}): 3265 (br, 2NH), 3101 (C—H aromatic), 2931, 2872 (C—H aliphatic), 1703 (C═O imide) and 1668 (C═O amide); ^{1}H NMR (DMSO-d_6) δ ppm: 1.95–2.07 (m, 2H, **CH$_2$**CH of piperidine), 2.48–2.51 (m, 1H, **CH$_2$**CO of piperidine), 2.68–2.77 (m, 1H, **CH$_2$**CO of piperidine), 4.20 (s, 2H, **CH$_2$**CO), 4.57–4.64 (m, 1H, **CH**CO), 7.65–7.68 (d, 2H, C-3 and C-5 phenyl, J = 12 Hz), 7.98–8.00 (d, 2H, J = 8.2 Hz, C-2 and C-6 phenyl,), 8.73–8.75 (d, 1H, J = 8.0 Hz, **NH**CO, D_2O exchangeable), 10.86 (s, 1H, CO**NH**CO, D_2O exchangeable); ^{13}C NMR (DMSO-d_6, 100 MHz) δ (ppm): 24.58, 31.26, 36.01, 50.15, 122.37, 128.69(2C), 130.05(2C), 137.18, 164.01, 164.81, 166.66, 172.20, 173.30; Anal. Calcd. for $C_{15}H_{13}ClN_4O_4S$ (380.80): C, 47.31; H, 3.44; N, 14.71. Found: C, 47.09; H, 3.49; N, 14.68%.

*4.1.3.5. N-(2,6-Dioxopiperidin-3-yl)-2-[(5-(4-nitrophenyl)-1,3,4-oxadiazol-2-yl)thio] Acetamide (**42$_e$**).* Faint green crystal (yield, 87%); m.p. = 276–278 °**C**. IR (KBr, cm^{-1}): 3277 (br, 2NH), 3095 (C—H aromatic), 2928, 2864 (C—H aliphatic), 1707 (C═O imide) and 1661 (C═O amide); ^{1}H NMR (DMSO-d_6) δ ppm: 1.92–1.97 (m, 2H, **CH$_2$**CH of piperidine), 2.47–2.50 (m, 1H, **CH$_2$**CO of piperidine), 2.68–2.77 (m, 1H, **CH$_2$**CO of piperidine), 4.22 (m, 2H, **CH$_2$**CO), 4.57–4.64 (m, 1H, **CH**CO), 8.23–8.25 (d, 2H, J = 8 *Hz*, C-2 and C-6 phenyl), 8.39–8.42 (d, 2H, C-3 and C-5 phenyl, J = 12 Hz), 8.75–8.77 (d, 1H, J = 8 Hz, NHCO, D_2O exchangeable), 10.85 (s, 1H, CONHCO, D_2O exchangeable); Anal. Calcd. for $C_{15}H_{13}N_5O_6S$ (391.36): C, 46.04; H, 3.35; N, 17.90. Found: C, 46.32; H, 3.55; N, 18.21%.

*4.1.3.6. 2-[(5-(4-Aminophenyl)-1,3,4-oxadiazol-2-yl)thio]-N-(2,6-dioxopiperidin-3-yl)acetamide (**42$_f$**).* Orange crystal (yield, 87%); m.p. = 255–257 °**C**. IR (KBr, cm^{-1}): 3360, 3277 (2NH), 3092 (C—H aromatic), 2884 (C—H aliphatic), 1706 (C═O imide) and 1635 (C═O amide); ^{1}H NMR (DMSO-d_6) δ ppm: 1.87–1.93 (m, 2H, **CH$_2$**CH of piperidine), 2.44–2.48 (m, 1H, **CH$_2$**CO of piperidine), 2.65–2.87 (m, 1H, **CH$_2$**CO of piperidine), 4.09 (s, 2H, **CH$_2$**CO), 4.53–4.60 (m, 1H, **CH**CO), 5.91 (s, 2H, NH_2, D_2O exchangeable), 6.62–6.64 (d, 2H, C-3 and C-5 phenyl, J = 8.2 Hz), 7.58–7.60 (d, 2H, C-2 and C-6 phenyl, J = 8.3 Hz), 8.65–8.67 (d, 1H, J = 8.0 Hz, NHCO, D_2O exchangeable), 10.82 (s, 1H, CONHCO, D_2O exchangeable); ^{13}C NMR (DMSO-d_6, 100 MHz) δ (ppm): 24.60, 31.25, 36.03, 50.13, 109.84, 114.00(2C), 128.42(2C), 152.81, 161.36, 166.42, 166.83, 172.20, 173.32; Anal. Calcd. for $C_{15}H_{15}N_5O_4S$ (361.38): C, 49.86; H, 4.18; N, 19.38. Found: C, 50.08; H, 4.39; N, 19.62%.

*4.1.3.7. N-(2,6-Dioxopiperidin-3-yl)-2-[(5-(pyridin-2-yl)-1,3,4-oxadiazol-2-yl)thio] Acetamide (**42$_g$**).* white crystal (yield, 82%); m.p. = 173–175 °**C**. IR (KBr, cm^{-1}): 3308, 3219 (2NH), 3091 (C—H aromatic), 2910 (C—H aliphatic), and 1689 (C═O amide); ^{1}H NMR (DMSO-d_6) δ ppm: 1.95–1.98 (m, 2H, **CH$_2$**CH of piperidine), 2.48–2.51 (m, 1H, **CH$_2$**CO of piperidine), 2.68–2.79 (m, 1H, **CH$_2$**CO of piperidine), 4.21 (s, 2H, **CH$_2$**CO), 4.59–4.65 (m, 1H, **CH**CO), 7.58–7.62 (dd, 1H, C-5 pyridine, J = 8 Hz), 8.04–8.08 (dd, 1H, C-4 pyridine, J = 8 Hz), 8.11–8.13 (d, 1H, C-3 pyridine, J = 8 *Hz*), 8.70–8.72 (d, 1H, J = 8 Hz, **NH**CO, D_2O exchangeable), 8.72–8.74 (d, 1H, C-6 pyridine, J = 8 Hz), 10.84 (s, 1H, CO**NH**CO, D_2O exchangeable); Anal. Calcd. for $C_{14}H_{13}N_5O_4S$ (347.35): C, 48.41; H, 3.77; N, 20.16. Found: C, 48.69; H, 3.88; N, 20.31%.

*4.1.3.8. N-(2,6-Dioxopiperidin-3-yl)-2-[(5-(pyridin-3-yl)-1,3,4-oxadiazol-2-yl)thio] Acetamide (**42$_h$**).* Greenish white crystal (yield, 82%); m.p. = 176–178 °**C**. IR (KBr, cm^{-1}): 3286 (br, 2NH), 3048, 3004 (C—H aromatic), 2923 (C—H aliphatic), 1703 (C═O imide) and 1673 (C═O amide); ^{1}H NMR (DMSO-d_6) δ ppm: 1.94–1.97 (m, 2H, **CH$_2$**CH of piperidine), 2.46–2.51 (m, 1H, **CH$_2$**CO of piperidine), 2.67–2.77 (m, 1H, **CH$_2$**CO of piperidine), 4.22 (m, 2H, **CH$_2$**CO), 4.57–4.63 (m, 1H, **CH**CO), 7.63–7.66 (dd, 1H, J = 4 *Hz* & 8 Hz, C-5 pyridine), 8.35–8.38 (d, 1H, J = 12 Hz, **NH**CO, D_2O exchangeable), 8.74–8.76 (d, 1H, J = 8 Hz, C-4 pyridine), 8.79–8.81(d, 1H, J = 8 Hz, C-6 pyridine), 9.15 (s, 1H, C-2 pyridine), 10.85 (s, 1H, CO**NH**CO, D_2O exchangeable); MS (m/z): 347 (M+, 51.34%), 49 (100%, base peak), 276 (22.31%), 149 (31.08%), 143 (30.46%), 121 (59.73%), 104 (67.68%), 97 (50.39%), 79 (73.70%), 66 (69.14%); Anal. Calcd. for $C_{14}H_{13}N_5O_4S$ (347.35): C, 48.41; H, 3.77; N, 20.16. Found: C, 48.52; H, 3.97; N, 20.29%.

*4.1.3.9. N-(2,6-Dioxopiperidin-3-yl)-2-[(5-(pyridin-4-yl)-1,3,4-oxadiazol-2-yl)thio] Acetamide (**42$_i$**).* Bluish crystal (yield, 89%); m.p. = 169–171 °**C**. IR (KBr, cm^{-1}): 3295 (br, 2NH), 2998 (C—H aromatic), 2917 (C—H aliphatic), 1708 (C═O imide) and 1653 (C═O amide); ^{1}H NMR (DMSO-d_6) δ ppm: 1.94–1.98 (m, 2H, **CH$_2$**CH of piperidine), 2.49–2.51 (m, 1H, **CH$_2$**CO of piperidine), 2.68–2.75 (m, 1H, **CH$_2$**CO of piperidine), 4.23 (s, 2H, **CH$_2$**CO), 4.59–4.63 (m, 1H, **CH**CO), 7.91–7.93 (d, 2H, C-3 and C-5 pyridine, J = 8.2 Hz), 8.74–8.76 (d, 1H, J = 8 Hz, **NH**CO, D_2O exchangeable), 8.80–8.82 (d, 2H, J = 8.1 Hz, C-2 and C-6 pyridine), 10.84 (s, 1H, CO**NH**CO, D_2O exchangeable); Anal. Calcd. for $C_{14}H_{13}N_5O_4S$ (347.35): C, 48.41; H, 3.77; N, 20.16. Found: C, 48.59; H, 4.02; N, 20.42%.

4.2. Biological testing

4.2.1. In vitro anti-proliferative activities

Anti-proliferative activity screening of the synthesized compounds was performed against four human cancer cell lines: hepatocellular carcinoma (HepG-2), colorectal carcinoma (HCT-116), prostate cancer (PC3), and mammary gland cancer (MCF-7), using MTT assay [78–81] as follows:

The cells were cultured in RPMI-1640 medium with 10% fetal bovine serum. Penicillin (100 units/ml) and streptomycin (100 μg/ml) were added at 37 C in a 5% CO_2 incubator. The cells were seeded in a 96-well plate at a density of $1.0x10^4$ cells/well. at 37 C for 48 h under 5% CO_2. After incubation the cells were treated with different concentration of the synthesized compounds and incubated for 24 h. Then, 20 μL of MTT solution of a concentration of 5 mg/ml was added and incubated for 4 h. DMSO (100 μL) was added into each well to dissolve the formed purple formazan. The color intensity was measured and recorded at absorbance of 570 nm using a plate reader (EXL 800, USA). The percentage of cell viability in was calculated as (A570 of treated samples/A570 of untreated sample) X 100. Results for IC_{50}values of the tested compounds were summarized in Table 1.

4.2.2. Supernatant preparation

Cell culture supernatants were prepared from HCT-116 cell line. Cells were cultured in RPMI 1640 medium supplemented with 10% heat-inactivated fetal bovine serum (FBS) having 100 U/ml of penicillin and 50 μg/ml of streptomycin at 37 °C in a humidified 5% CO_2/air mixture. The candidate compounds and thalidomide were dissolved in DMSO as a stock solution at 100 mmol/L and diluted with an FBS-free medium to achieve the designated concentrations (10 μM). The same concentration of DMSO without any compounds was used as a control. The HCT-116 cells were cultured onto 6-well plates (1x106 cells/ well), allowed to adhere for 24 h followed by treatment with the tested compounds. After 72 h, the media was collected and centrifuged for 15 min at 5000 rpm and equal volume of cell culture supernatants were collected and utilized for immunoassay using different kits [82].

4.2.2.1. Estimation of TNF-α, CASP8, and VEGF in HCT-116 supernatant. The levels of TNF-α, CASP8, and VEGF in cell culture supernatants were estimated by ELISA technique using commercially available matched paired antibodies (R&D Systems Inc., Minneapolis,

MN) according to reported procedure [83,84].

4.2.3. Cell lysate preparation

The tested compounds and thalidomide were incubated for 72 h with HCT-116 cells. Then, the cells were treated with trypsin/EDTA solution (0.25 mM trypsin and 1 mM EDTA dissolved in a phosphate buffer). Cell lysate were washed three times with phosphate buffer saline (PBS, Sigma Chemical Company, St. Louis, MO, USA) and lysed by three repetitive freezing/thawing cycles (thawing at 37 °C for 2 min and freezing at –80 °C for 15 min), followed by homogenization of the cells by passing through a 20G needle [85].

4.2.3.1. Estimation of nuclear factor kappa-B P65 (NF-κB P65) in HCT-116 cell lysate. The cell lysate samples were applied to the microtiter plates in a concentration of 50 µL/well. The plates were incubated at 37 °C for 1 h, then kept at 4 °C for 12 h in a humidified chamber. Next, the cell lysate was extracted from the wells and the plates were washed three times with a buffer (PBS/0.05%Tween-20). Blocking buffer (PBS/0.05%Tween-20/5% FBS) (200 µL) was added to each well and incubated at 37 °C for 1.5 h then washed. Anti-rabbit NF-κB *P*65 polyclonal antibody was dispensed as 50 µL/well and incubated for 2 h at 37 °C. The plates were washed and incubated for 1 h with 50 µL/well of diluted polyclonal goat anti-rabbit-peroxidase conjugate (1:1000). After that, the plates were washed four times followed by addition of TMB and H_2O_2 in equal volume (50 µL/well). After the development of color, 50 µL of stopping buffer (1 M HCl) were added per well. The absorbance was measured at 450 nm using the ELISA plate reader (FLUOstar OPTIMA) [85].

4.2.4. Cell cycle analysis

HCT-116 cells were seeded at density of 2×10^5 cells per well and incubated in six-well plates for 24 h. Fetal bovine serum (FBS, 10%) was applied after incubation of cells at 37 °C and 5% CO_2. The medium was substituted with (DMSO 1% v/v) containing the compound $\mathbf{20_f}$ 10 µM, then incubated for 48 h, washed with saline buffered with cold phosphate (PBS), fixed with 70% ethanol, rinsed with PBS then stained with the DNA fluorochrome PI, kept for 15 min at 37 °C. Then samples were analyzed with a FACS Caliber flow cytometer [86,87].

4.2.5. Annexin V-FITC apoptosis assay

Annexin V-FITC / PI apoptosis detection kit was used to analyze the effect of the most cytotoxic compound $\mathbf{42_f}$ on apoptosis induction. In this experiment, HCT-116 cells were stained with Annexin V fluorescein isothiocyanate (FITC) and counterstained with propidium iodide (PI). Then, HCT-116 cells in a density of 2×10^5 per well were incubated with compound $\mathbf{42_f}$ (10 µM) for 48 h. Next, the cells were trypsinized, washed with phosphate-buffered saline (PBS), and stained for 15 min at 37 °C in the dark. Finally, FACS Caliber flow cytometer was used in analysis process [88,89].

4.2.6. Statistical analysis

The statistical analyses were performed using GraphPad Prism 6.01 MM. Data were presented as means with corresponding SE. Comparisons between different groups were performed by one-way analysis of variance (ANOVA). Tukey's test was used as a post-hoc test. Correlation among variables was deter-mined using Pearson's correlation test. The level of significance was set at $P < 0.05$.

Declaration of Competing Interest

The authors declare that they have no known competing financial interests or personal relationships that could have appeared to influence the work reported in this paper.

Acknowledgement

Authors are thankful to the team of Pharmacology & Toxicology Department, Faculty of pharmacy (Boys), Al-Azhar University, Cairo, Egypt and the team of Biochemistry Department, Faculty of medicine, Cairo University, Cairo, Egypt for providing laboratory facilities for biological activity.

Appendix A. Supplementary material

Supplementary data to this article can be found online at https://doi.org/10.1016/j.bioorg.2020.104218.

References

[1] J.B. Marriott, G. Muller, A.G. Dalgleish, Thalidomide as an emerging immunotherapeutic agent, Immunol. Today 20 (12) (1999) 538–540.
[2] N. Vargesson, Thalidomide-induced teratogenesis: History and mechanisms, Birth Defects Res. Part C: Embryo Today: Rev. 105 (2) (2015) 140–156.
[3] T. Ito, H. Ando, H. Handa, Teratogenic effects of thalidomide: molecular mechanisms, Cell. Mol. Life Sci. 68 (9) (2011) 1569–1579.
[4] T. Stephens, R. Brynner, Dark Remedy: The Impact of Thalidomide And its Revival as A Vital Medicine, Basic Books, 2009.
[5] S. Sleijfer, W.H. Kruit, G. Stoter, Thalidomide in solid tumours: the resurrection of an old drug, Eur. J. Cancer 40 (16) (2004) 2377–2382.
[6] J.H. Kim, A.R. Scialli, Thalidomide: the tragedy of birth defects and the effective treatment of disease, Toxicol. Sci. 122 (1) (2011) 1–6.
[7] I. Ali, W.A. Wani, K. Saleem, A. Haque, Thalidomide: a banned drug resurged into future anticancer drug, Curr. Drug Therapy 7 (1) (2012) 13–23.
[8] J.B. Bartlett, K. Dredge, A.G. Dalgleish, The evolution of thalidomide and its IMiD derivatives as anticancer agents, Nat. Rev. Cancer 4 (4) (2004) 314.
[9] P.A. Haslett, P. Roche, C.R. Butlin, M. Macdonald, N. Shrestha, R. Manandhar, J. LeMaster, R. Hawksworth, M. Shah, A.S. Lubinsky, Effective treatment of erythema nodosum leprosum with thalidomide is associated with immune stimulation, J. Infect. Dis. 192 (12) (2005) 2045–2053.
[10] M. Dimopoulos, K. Zervas, G. Kouvatseas, E. Galani, V. Grigoraki, C. Kiamouris, E. Vervessou, E. Samantas, C. Papadimitriou, O. Ecomomou, Thalidomide and dexamethasone combination for refractory multiple myeloma, Ann. Oncol. 12 (7) (2001) 991–995.
[11] J. Folkman, Angiogenesis-dependent diseases, Seminars in oncology, Elsevier, 2001, pp. 536–542.
[12] R. Knight, IMiDs: a novel class of immunomodulators, Seminars in oncology, Elsevier, 2005, pp. 24–30.
[13] M. Melchert, A. List, The thalidomide saga, Int. J. Biochem. Cell Biol. 39 (7–8) (2007) 1489–1499.
[14] K.M. Cook, W.D. Figg, Angiogenesis inhibitors: current strategies and future prospects, CA Cancer J. Clin. 60 (4) (2010) 222–243.
[15] A.C.L. Leite, F.F. Barbosa, M.V. de Oliveira Cardoso, D.R. Moreira, L.C.D. Coêlho, E. B. da Silva, G.B. de Oliveira Filho, V.M.O. de Souza, V.R.A. Pereira, L.d.C. Reis, Phthaloyl amino acids as anti-inflammatory and immunomodulatory prototypes, Medicinal Chem. Res. 23(4) (2014) 1701–1708.
[16] A.L. Ruchelman, H.-W. Man, W. Zhang, R. Chen, L. Capone, J. Kang, A. Parton, L. Corral, P.H. Schafer, D. Babusis, Isosteric analogs of lenalidomide and pomalidomide: Synthesis and biological activity, Bioorg. Med. Chem. Lett. 23 (1) (2013) 360–365.
[17] S.K. Teo, Properties of thalidomide and its analogues: implications for anticancer therapy, AAPS J. 7 (1) (2005) E14–E19.
[18] R. Suppiah, J.G. Srkalovic, M.A. Hussein, Immunomodulatory analogues of thalidomide in the treatment of multiple myeloma, Clin. Lymphoma Myeloma 6 (4) (2006) 301–305.
[19] E. Terpos, N. Kanellias, D. Christoulas, E. Kastritis, M.A. Dimopoulos, Pomalidomide: a novel drug to treat relapsed and refractory multiple myeloma, OncoTargets Therapy 6 (2013) 531.
[20] S. Zhou, F. Wang, T.-C. Hsieh, J.M. Wu, E. Wu, Thalidomide–a notorious sedative to a wonder anticancer drug, Curr. Med. Chem. 20 (33) (2013) 4102–4108.
[21] W.D. Figg, W. Dahut, P. Duray, M. Hamilton, A. Tompkins, S.M. Steinberg, E. Jones, A. Premkumar, W.M. Linehan, M.K. Floeter, A randomized phase II trial of thalidomide, an angiogenesis inhibitor, in patients with androgen-independent prostate cancer, Clin. Cancer Res. 7 (7) (2001) 1888–1893.
[22] C.M. de Souza, L.F. de Carvalho, T. da Silva Vieira, A.C.A. e Silva, M.T.P. Lopes, M.A.N.D. Ferreira, S.P. Andrade, G.D. Cassali, Thalidomide attenuates mammary cancer associated-inflammation, angiogenesis and tumor growth in mice, Biomed. Pharmacother. 66 (7) (2012) 491–498.
[23] S. Ng, M. Brown, W. Figg, Thalidomide, an antiangiogenic agent with clinical activity in cancer, Biomed. Pharmacother. 56 (4) (2002) 194–199.
[24] T. Eisen, C. Boshoff, I. Mak, F. Sapunar, M. Vaughan, L. Pyle, S. Johnston, R. Ahern, I. Smith, M. Gore, Continuous low dose thalidomide: a phase II study in advanced melanoma, renal cell, ovarian and breast cancer, Br. J. Cancer 82 (4) (2000) 812.
[25] K.A. Varker, J. Campbell, M.H. Shah, Phase II study of thalidomide in patients with metastatic carcinoid and islet cell tumors, Cancer Chemother. Pharmacol. 61 (4) (2008) 661–668.

[26] S.-F. Ang, S.-H. Tan, H.-C. Toh, D.Y. Poon, S.Y. Ong, K.-F. Foo, S.-P. Choo, Activity of thalidomide and capecitabine in patients with advanced hepatocellular carcinoma, Am. J. Clin. Oncol. 35 (3) (2012) 222–227.
[27] R. Duncan, Polymer conjugates as anticancer nanomedicines, Nat. Rev. Cancer 6 (9) (2006) 688.
[28] G. Barosi, M. Elliott, L. Canepa, F. Ballerini, P.P. Piccaluga, G. Visani, M. Marchetti, G. Pozzato, F. Zorat, A. Tefferi, Thalidomide in myelofibrosis with myeloid metaplasia: a pooled-analysis of individual patient data from five studies, Leukemia Lymphoma 43 (12) (2002) 2301–2307.
[29] M.B. Steins, T. Padró, R. Bieker, S. Ruiz, M. Kropff, J. Kienast, T. Kessler, T. Buechner, W.E. Berdel, R.M. Mesters, Efficacy and safety of thalidomide in patients with acute myeloid leukemia, Blood 99 (3) (2002) 834–839.
[30] A.K. Gandhi, J. Kang, C.G. Havens, T. Conklin, Y. Ning, L. Wu, T. Ito, H. Ando, M.F. Waldman, A. Thakurta, Immunomodulatory agents lenalidomide and pomalidomide co-stimulate T cells by inducing degradation of T cell repressors I karos and A iolos via modulation of the E 3 ubiquitin ligase complex CRL 4 CRBN, Br. J. Haematol. 164 (6) (2014) 811–821.
[31] P. Bodera, W. Stankiewicz, Immunomodulatory properties of thalidomide analogs: pomalidomide and lenalidomide, experimental and therapeutic applications, Recent Pat. Endocr., Metab. Immune Drug Discov. 5 (3) (2011) 192–196.
[32] J.W. Adlard, Thalidomide in the treatment of cancer, Anticancer Drugs 11 (10) (2000) 787–791.
[33] K.C. Anderson, Lenalidomide and thalidomide: mechanisms of action—similarities and differences, Seminars Hematol. Elsevier (2005) S3–S8.
[34] Y. Dai, F. Jin, W. Li, J.G. Turner, Novel mechanisms of action for immunomodulatory drugs (IMiDs) against multiple myeloma: from a tragedy to a therapy, Int. J. Hematol. Therapy 2 (1) (2015).
[35] T. Reske, M. Fulciniti, N.C. Munshi, Mechanism of action of immunomodulatory agents in multiple myeloma, Med. Oncol. 27 (1) (2010) 7–13.
[36] A. Avigdor, P. Raanani, I. Levi, I. Hardan, I. Ben-Bassat, Extramedullary progression despite a good response in the bone marrow in patients treated with thalidomide for multiple myeloma, Leukemia Lymphoma 42 (4) (2001) 683–687.
[37] W.M. Eldehna, M.F. Abo-Ashour, A. Nocentini, P. Gratteri, I.H. Eissa, M. Fares, O.E. Ismael, H.A. Ghabbour, M.M. Elaasser, H.A. Abdel-Aziz, Novel 4/3-((4-oxo-5-(2-oxoindolin-3-ylidene) thiazolidin-2-ylidene) amino) benzenesulfonamides: Synthesis, carbonic anhydrase inhibitory activity, anticancer activity and molecular modelling studies, Eur. J. Med. Chem. 139 (2017) 250–262.
[38] A.A. Gaber, A.H. Bayoumi, A.M. El-morsy, F.F. Sherbiny, A.B. Mehany, I.H. Eissa, Design, synthesis and anticancer evaluation of 1H-pyrazolo [3, 4-d] pyrimidine derivatives as potent EGFR WT and EGFR T790M inhibitors and apoptosis inducers, Bioorg. Chem. (2018).
[39] A.M. El-Naggar, M.M. Abou-El-Regal, S.A. El-Metwally, F.F. Sherbiny, I.H. Eissa, Synthesis, characterization and molecular docking studies of thiouracil derivatives as potent thymidylate synthase inhibitors and potential anticancer agents, Mol. Diversity 21 (4) (2017) 967–983.
[40] S.A. Elmetwally, K.F. Saied, I.H. Eissa, E.B. Elkaeed, Design, synthesis and anticancer evaluation of thieno [2, 3-d] pyrimidine derivatives as dual EGFR/HER2 inhibitors and apoptosis inducers, Bioorg. Chem. 88 (2019) 102944.
[41] H.A. Mahdy, M.K. Ibrahim, A.M. Metwaly, A. Belal, A.B. Mehany, K.M. El-Gamal, A. El-Sharkawy, M.A. Elhendawy, M.M. Radwan, M.A. Elsohly, Design, synthesis, molecular modeling, in vivo studies and anticancer evaluation of quinazolin-4 (3H)-one derivatives as potential VEGFR-2 inhibitors and apoptosis inducers, Bioorg. Chem. (2019) 103422.
[42] I.H. Eissa, A.M. El-Naggar, M.A. El-Hashash, Design, synthesis, molecular modeling and biological evaluation of novel 1H-pyrazolo [3, 4-b] pyridine derivatives as potential anticancer agents, Bioorg. Chem. 67 (2016) 43–56.
[43] I.H. Eissa, A.M. El-Naggar, N.E. El-Sattar, A.S. Youssef, Design and discovery of novel quinoxaline derivatives as dual DNA intercalators and topoisomerase II inhibitors, Anti-Cancer Agents in Medicinal Chemistry (Formerly Current Medicinal Chemistry-Anti-Cancer Agents) 18 (2) (2018) 195–209.
[44] M. Ibrahim, M. Taghour, A. Metwaly, A. Belal, A. Mehany, M. Elhendawy, M. Radwan, A. Yassin, N. El-Deeb, E. Hafez, Design, synthesis, molecular modeling and anti-proliferative evaluation of novel quinoxaline derivatives as potential DNA intercalators and topoisomerase II inhibitors, Eur. J. Med. Chem. (2018).
[45] I.H. Eissa, A.M. Metwaly, A. Belal, A.B. Mehany, R.R. Ayyad, K. El-Adl, H.A. Mahdy, M.S. Taghour, K.M. El-Gamal, M.E. El-Sawah, Discovery and antiproliferative evaluation of new quinoxalines as potential DNA intercalators and topoisomerase II inhibitors, Arch. Pharm. 352 (11) (2019) 1900123.
[46] A.G.A. El-Helby, H. Sakr, I.H. Eissa, H. Abulkhair, A.A. Al-Karmalawy, K. El-Adl, Design, synthesis, molecular docking, and anticancer activity of benzoxazole derivatives as VEGFR-2 inhibitors, Arch. Pharm. 352 (10) (2019) 1900113.
[47] A.M. El-Naggar, I.H. Eissa, A. Belal, A.A. El-Sayed, Design, eco-friendly synthesis, molecular modeling and anticancer evaluation of thiazol-5 (4 H)-ones as potential tubulin polymerization inhibitors targeting the colchicine binding site, RSC Adv. 10 (5) (2020) 2791–2811.
[48] G.W. Muller, L.G. Corral, M.G. Shire, H. Wang, A. Moreira, G. Kaplan, D.I. Stirling, Structural modifications of thalidomide produce analogs with enhanced tumor necrosis factor inhibitory activity, J. Med. Chem. 39 (17) (1996) 3238–3240.
[49] S.M. Capitosti, T.P. Hansen, M.L. Brown, Thalidomide analogues demonstrate dual inhibition of both angiogenesis and prostate cancer, Bioorg. Med. Chem. 12 (2) (2004) 327–336.
[50] T. Noguchi, H. Fujimoto, H. Sano, A. Miyajima, H. Miyachi, Y. Hashimoto, Angiogenesis inhibitors derived from thalidomide, Bioorg. Med. Chem. Lett. 15 (24) (2005) 5509–5513.
[51] S.G. Stewart, D. Spagnolo, M.E. Polomska, M. Sin, M. Karimi, L.J. Abraham, Synthesis and TNF expression inhibitory properties of new thalidomide analogues derived via Heck cross coupling, Bioorg. Med. Chem. Lett. 17 (21) (2007) 5819–5824.
[52] T. Wang, Y.H. Zhang, S. Yu, H. Ji, Y.S. Lai, S.X. Peng, Synthesis and biological evaluation of novel thalidomide analogues as potential anticancer drugs, Chin. Chem. Lett. 19 (8) (2008) 928–930.
[53] M.A.-H. Zahran, T.A.-R. Salem, R.M. Samaka, H.S. Agwa, A.R. Awad, Design, synthesis and antitumor evaluation of novel thalidomide dithiocarbamate and dithioate analogs against Ehrlich ascites carcinoma-induced solid tumor in Swiss albino mice, Bioorg. Med. Chem. 16 (22) (2008) 9708–9718.
[54] M.F. Braña, N. Acero, L. Anorbe, D.M. Mingarro, F. Llinares, G. Domínguez, Discovering a new analogue of thalidomide which may be used as a potent modulator of TNF-α production, Eur. J. Med. Chem. 44 (9) (2009) 3533–3542.
[55] C. Chaulet, C. Croix, D. Alagille, S. Normand, A. Delwail, L. Favot, J.-C. Lecron, M.-C. Viaud-Massuard, Design, synthesis and biological evaluation of new thalidomide analogues as TNF-α and IL-6 production inhibitors, Bioorg. Med. Chem. Lett. 21 (3) (2011) 1019–1022.
[56] L. Mazzoccoli, S.H. Cadoso, G.W. Amarante, M.V. de Souza, R. Domingues, M.A. Machado, M.V. de Almeida, H.C. Teixeira, Novel thalidomide analogues from diamines inhibit pro-inflammatory cytokine production and CD80 expression while enhancing IL-10, Biomed. Pharmacother. 66 (5) (2012) 323–329.
[57] S. Nagarajan, S. Majumder, U. Sharma, S. Rajendran, N. Kumar, S. Chatterjee, B. Singh, Synthesis and anti-angiogenic activity of benzothiazole, benzimidazole containing phthalimide derivatives, Bioorg. Med. Chem. Lett. 23 (1) (2013) 287–290.
[58] P.M. Da Costa, M.P. da Costa, A.A. Carvalho, S.M.T. Cavalcanti, M.V. de Oliveira Cardoso, G.B. de Oliveira Filho, D. de Araújo Viana, F.V. Fechine-Jamacaru, A.C.L. Leite, M.O. de Moraes, Improvement of in vivo anticancer and antiangiogenic potential of thalidomide derivatives, Chemico-biological Interact. 239 (2015) 174–183.
[59] M.V. de Oliveira Cardoso, D.R.M. Moreira, G.B. Oliveira Filho, S.M.T. Cavalcanti, L.C.D. Coelho, J.W.P. Espíndola, L.R. Gonzalez, M.M. Rabello, M.Z. Hernandes, P.M.P. Ferreira, Design, synthesis and structure–activity relationship of phthalimides endowed with dual antiproliferative and immunomodulatory activities, Eur. J. Med. Chem. 96 (2015) 491–503.
[60] S. Bajaj, V. Asati, J. Singh, P.P. Roy, 1, 3, 4-Oxadiazoles: an emerging scaffold to target growth factors, enzymes and kinases as anticancer agents, Eur. J. Med. Chem. 97 (2015) 124–141.
[61] W. Caneschi, K.B. Enes, C.C. de Mendonça, F. de Souza Fernandes, F.B. Miguel, J. da Silva Martins, M. Le Hyaric, R.R. Pinho, L.M. Duarte, M.A.L. de Oliveira, Synthesis and anticancer evaluation of new lipophilic 1, 2, 4 and 1, 3, 4-oxadiazoles, Eur. J. Med. Chem. 165 (2019) 18–30.
[62] H. El-Kashef, G. Badr, N.A. El-Maali, D. Sayed, P. Melnyk, N. Lebegue, R.A. El-Khalek, Synthesis of a novel series of (Z)-3, 5-disubstituted thiazolidine-2, 4-diones as promising anti-breast cancer agents, Bioorg. Chem. (2020) 103569.
[63] C. Viegas-Junior, A. Danuello, V. da Silva Bolzani, E.J. Barreiro, C.A.M. Fraga, Molecular hybridization: a useful tool in the design of new drug prototypes, Curr. Med. Chem. 14 (17) (2007) 1829–1852.
[64] M.A. El-Zahabi, E.R. Elbendary, F.H. Bamanie, M.F. Radwan, S.A. Ghareib, I.H. Eissa, Design, synthesis, molecular modeling and anti-hyperglycemic evaluation of phthalimide-sulfonylurea hybrids as PPARγ and SUR agonists, Bioorg. Chem. 91 (2019) 103115.
[65] G. Bruno, L. Costantino, C. Curinga, R. Maccari, F. Monforte, F. Nicolo, R. Ottana, M. Vigorita, Synthesis and aldose reductase inhibitory activity of 5-arylidene-2, 4-thiazolidinediones, Bioorg. Med. Chem. 10 (4) (2002) 1077–1084.
[66] R. Maccari, R. Ottanà, R. Ciurleo, M.G. Vigorita, D. Rakowitz, T. Steindl, T. Langer, Evaluation of in vitro aldose redutase inhibitory activity of 5-arylidene-2, 4-thiazolidinediones, Bioorg. Med. Chem. Lett. 17 (14) (2007) 3886–3893.
[67] K.M. El-Gamal, A.M. El-Morsy, A.M. Saad, I.H. Eissa, M. Alswah, Synthesis, docking, QSAR, ADMET and antimicrobial evaluation of new quinoline-3-carbonitrile derivatives as potential DNA-gyrase inhibitors, J. Mol. Struct. 1166 (2018) 15–33.
[68] M.K. Ibrahim, I.H. Eissa, A.E. Abdallah, A.M. Metwaly, M. Radwan, M. ElSohly, Design, synthesis, molecular modeling and anti-hyperglycemic evaluation of novel quinoxaline derivatives as potential PPARγ and SUR agonists, Bioorg. Med. Chem. 25 (4) (2017) 1496–1513.
[69] M.K. Ibrahim, I.H. Eissa, M.S. Alesawy, A.M. Metwaly, M.M. Radwan, M.A. ElSohly, Design, synthesis, molecular modeling and anti-hyperglycemic evaluation of quinazolin-4 (3H)-one derivatives as potential PPARγ and SUR agonists, Bioorg. Med. Chem. 25 (17) (2017) 4723–4744.
[70] K. Gholivand, H. Mostaanzadeh, Z. Shariatinia, N. Oroujzadeh, Syntheses, crystal structures and dynamic 1HNMR study of diastereotopic CH2 protons in several new phosphoric triamides, Main Group Chem. Taylor & Francis (2006) 95–106.
[71] J.A. Aizina, I.B. Rozentsveig, G.G. Levkovskaya, A novel synthesis of chloroacetamide derivatives via C-amidoalkylation of aromatics by 2-chloro-N-(2, 2, 2-trichloro-1-hydroxyethyl) acetamide, Arkivoc 8 (2011) 192–199.
[72] J.A. DaSilva, C. Barríab, C. Jullianb, P. Navarreteb, L. NúñezVergaraa, J. Squellaa, Unexpected diastereotopic behaviour in the 1H NMR spectrum of 1, 4-dihydropyridine derivatives triggered by chiral and prochiralcentres, J. Braz. Chem. Soc. 16 (2005) 112.
[73] Z. Shi, Z. Zhao, M. Huang, X. Fu, Ultrasound-assisted, one-pot, three-component synthesis and antibacterial activities of novel indole derivatives containing 1, 3, 4-oxadiazole and 1, 2, 4-triazole moieties, C. R. Chim. 18 (12) (2015) 1320–1327.
[74] S.J. Gilani, S.A. Khan, N. Siddiqui, Synthesis and pharmacological evaluation of condensed heterocyclic 6-substituted 1, 2, 4-triazolo-[3, 4-b]-1, 3, 4-thiadiazole and 1, 3, 4-oxadiazole derivatives of isoniazid, Bioorg. Med. Chem. Lett. 20 (16) (2010) 4762–4765.
[75] E. Borenfreund, J.A. Puerner, Toxicity determined in vitro by morphological

alterations and neutral red absorption, Toxicol. Lett. 24 (2–3) (1985) 119–124.
[76] C. Riccardi, I. Nicoletti, Analysis of apoptosis by propidium iodide staining and flow cytometry, Nat. Protoc. 1 (3) (2006) 1458.
[77] A.G.A. El-Helby, H. Sakr, I.H. Eissa, A.A. Al-Karmalawy, K. El-Adl, Benzoxazole/benzothiazole-derived VEGFR-2 inhibitors: Design, synthesis, molecular docking, and anticancer evaluations, Arch. Pharm. 352 (12) (2019) 1900178.
[78] T. Mosmann, Rapid colorimetric assay for cellular growth and survival: application to proliferation and cytotoxicity assays, J. Immunol. Methods 65 (1–2) (1983) 55–63.
[79] F. Denizot, R. Lang, Rapid colorimetric assay for cell growth and survival: modifications to the tetrazolium dye procedure giving improved sensitivity and reliability, J. Immunol. Methods 89 (2) (1986) 271–277.
[80] M.I. Thabrew, R.D. Hughes, I.G. Mcfarlane, Screening of hepatoprotective plant components using a HepG2 cell cytotoxicity assay, J. Pharm. Pharmacol. 49 (11) (1997) 1132–1135.
[81] H. Almahli, E. Hadchity, M.Y. Jaballah, R. Daher, H.A. Ghabbour, M.M. Kabil, N.S. Al-shakliah, W.M. Eldehna, Development of novel synthesized phthalazinone-based PARP-1 inhibitors with apoptosis inducing mechanism in lung cancer, Bioorg. Chem. 77 (2018) 443–456.
[82] T. Inoue, K. Kibata, M. Suzuki, S. Nakamura, R. Motoda, K. Orita, Identification of a vascular endothelial growth factor (VEGF) antagonist, sFlt-1, from a human hematopoietic cell line NALM-16, FEBS Lett. 469 (1) (2000) 14–18.
[83] R.M. Talaat, Soluble angiogenesis factors in sera of Egyptian patients with hepatitis C virus infection: correlation with disease severity, Viral Immunol. 23 (2) (2010) 151–157.
[84] mybiosource.com/, MyBioSource ELISA Test Kits, 2019. https://www.mybiosource.com/human-elisa-kits/casp8/2513072#QLAPP_MBS2513072_TD (accessed May 2018)..
[85] R. Talaat, W. El-Sayed, H. Agwa, A. Gamal-Eldeen, S. Moawia, M. Zahran, Novel thalidomide analogs: Anti-angiogenic and apoptotic effects on Hep-G2 and MCF-7 cancer cell lines, Biomed. Aging Pathol. 4 (3) (2014) 179–189.
[86] J. Wang, M.J. Lenardo, Roles of caspases in apoptosis, development, and cytokine maturation revealed by homozygous gene deficiencies, J. Cell Sci. 113 (5) (2000) 753–757.
[87] W.M. Eldehna, G.S. Hassan, S.T. Al-Rashood, T. Al-Warhi, A.E. Altyar, H.M. Alkahtani, A.A. Almehizia, H.A. Abdel-Aziz, Synthesis and in vitro anticancer activity of certain novel 1-(2-methyl-6-arylpyridin-3-yl)-3-phenylureas as apoptosis-inducing agents, J. Enzyme Inhib. Med. Chem. 34 (1) (2019) 322–332.
[88] K.K.-W. Lo, T.K.-M. Lee, J.S.-Y. Lau, W.-L. Poon, S.-H. Cheng, Luminescent biological probes derived from ruthenium (II) estradiol polypyridine complexes, Inorg. Chem. 47 (1) (2008) 200–208.
[89] W.M. Eldehna, A. Nocentini, Z.M. Elsayed, T. Al-Warhi, N. Aljaeed, O.J. Alotaibi, M.M. Al-Sanea, H.A. Abdel-Aziz, C.T. Supuran, Benzofuran-based carboxylic acids as carbonic anhydrase inhibitors and antiproliferative agents against breast cancer, ACS Med. Chem. Lett. (2020).